Stem Cell Therapies – The Underlying Biology and Impact on Clinical Trials

F Dazzi

Stem Cell Biology, Department of Medicine, Imperial College, London, United Kingdom

SUMMARY

Stem cell therapies have raised enormous interest in the last decade. A large number of progenitors/stem cells have been identified from different sources and with different features that, at least *in vitro*, exhibit the ability to differentiate into tissues originating from one or more of the embryonic sheets. These findings have ignited a number of initiatives to test stem cells in pre-clinical models and in some cases in the clinical setting. In some circumstances therapeutic approaches have been proven beneficial although the mechanisms of action underlying their efficacy remain to be elucidated. There is not convincing evidence that stem cells *in vivo* act through a direct regenerative process, as is the case of haemopoietic stem cells infused after myeloablation. Similarly, the findings that progenitor/stem cells can improve functionality in tissues of different embryonic origin have not been confirmed. The studies conducted on mesenchymal stem cells (MSC) have provided an important lesson to clarify some of these issues. MSC are stromal progenitor cells characterised by their ability to differentiate into bone, adipocytes, chondrocytes, and skeletal myocytes. As such they have been initially tested in clinical situations of genetic bone disorder with some encouraging results. However, they have become very attractive because of the observation that they can produce a potent immunosuppressive and anti-inflammatory activity. MSC inhibit T-cell responses in vitro and in vivo by inducing a form of immunological "division arrest anergy" whereby T cells become unable to proliferate though partly maintaining their effector functions. MSC have also been shown to inhibit the differentiation and function of dendritic cells as well as the proliferation and antibody production of B lymphocyte. These properties have been exploited for the treatment of severe refractory graft-versus-host disease (GvHD) after allogeneic bone marrow transplantation with extremely encouraging results. Highly convincing was a phase II multicentre clinical trial demonstrating that MSC administered to 55 patients with steroid-resistant acute GvHD produced complete remission in 30 patients and measurable improvement in a further 9 patients. Remissions were durable, since responders experienced a higher overall survival 2 years after HSCT than non-responders. Our research has documented that the immunosuppressive activity of MSC is based on a prominent anti-proliferative effect associated with an anti-apoptotic activity that not only targets immune cells but can also rescue parenchymal cells from injury related death. The modalities by which MSC exert these functions are being unraveled, but a crucial aspect is that these properties are not constitutive of MSC, but require a 'licensing' step, provided by the microenvironment, in which macrophages are prominently involved. Furthermore, whilst macrophages 'license' MSC, activated MSC eventually recruit macrophages to mediate and amplify the same effects. We will discuss how this haemopoietic-mesenchymal stroma interaction can be identified in other tissues and extends its effects to the regulation of parenchymal stem cell renewal and differentiation. Dissecting the molecular pathways of such interaction will identify strategies to manipulate resident stem cells.

Foxg1: A Key Regulator of Neural Fate

B Martynoga, M Manuel, D J Price, J O Mason

Genes & Development Group, Centre for Integrative Physiology, University of Edinburgh, Hugh Robson Building, George Square, Edinburgh EH8 9XD, United Kingdom

SUMMARY

Understanding the mechanisms that regulate the embryonic development of the mammalian forebrain remains one of the greatest challenges facing contemporary biology. At early stages of forebrain development, a complex interplay between signalling proteins and transcription factors act to confer specific regional identities on emerging neurons. Understanding the mechanisms by which these molecules act will help guide experimental strategies to produce defined populations of neurons from embryonic stem cells, with obvious benefits for regenerative medicine. We have explored the function of the winged helix transcription factor Foxg1 in early development of the forebrain. *Foxg1*$^{-/-}$ mutant mice completely lack a ventral telencephalon and the dorsal telencephalon is abnormally small. Using a combination of approaches, we have shown that Foxg1 is required cell-autonomously in the ventral telencephalon both to allow progenitor cells to adopt correct identities and to respond appropriately to ventralising signals including Shh and FGF.

Mesenchymal Stem Cells Transplantation Protects Dopaminergic Neurons in the Substantia Nigra in Parkinson's Disease

S S W Tay

Department of Anatomy, Yong Loo Lin School of Medicine, National University of Singapore, Singapore 117597

SUMMARY

Recent research findings suggest that transplanted mesenchymal stem cells (MSCs) have immunomodulatory effects in the MPTP-induced mouse model of Parkinson's disease (PD). After MPTP-treatment, a significant loss of dopaminergic neurons, and decreased expressions of claudin 1, claudin 5 and occludin in the endothelia of blood vessels were observed in the substantia nigra pars compacta (SNc), indicating damage to the blood brain barrier (BBB). The upregulated expressions of mannose-binding lectins (MBL) in the liver and the infiltration of MBL into the SNc of MPTP-treated mice suggest that a compromise in the BBB, and the MBL-induced activation of microglia cytotoxicity may have stimulated the pathogenesis of MPTP-induced PD. Transplantation of MSCs into MPTP-treated mice led to a recovery of BBB integrity, the suppression of MBL expressions in the liver and their infiltration into the SNc,, as well as the suppression of microglial activities. Although transplanted MSCs successfully homed into the SNc with cues from cytokines and chemokines (released by activated microglia) and they also released TGF-β1, none of the transplanted MSCs have been found to transdifferentiate into dopaminergic neurons. It is hypothesized that transplanted MSCs released some as yet unknown factors into the micro-environment of the brain that help to reduce dopaminergic neuronal cell death resulting from MPTP toxicity by the suppression of MBL expressions in the liver, their infiltration into the SNc, as well as the inhibition of microglial cytotoxicity. The exact mechanism for the neuroprotection of dopaminergic neurons in the SNc by the homed MSCs after the onset of Parkinson's disease is still unknown. This research was supported by research grants R181-000-096-112 from the Academic Research Fund (ARF), National University of Singapore and R181-000-128-112 from the Ministry of Education, Singapore.

Stem Cell and Immune Tolerance

F Dazzi

Stem Cell Biology Section, Department of Medicine - Imperial College, London, United Kingdom.

SUMMARY

Stem cell therapies, pioneered for the treatment of malignancies in the form of bone marrow transplantation, have subsequently been tested and successfully employed also in autoimmune diseases (AD). Autologous haemopoietic stem cell transplantation (HSCT) has become a curative option for conditions with very poor prognosis in which targeted therapies have little or no effect. Although HSCT remains a non-specific approach, the knowledge gained in this field has led to the identification of new avenues. In fact, it has become evident that the therapeutic efficacy of HSCT cannot merely be the consequence to a high dose immunosuppression but rather the result of a resetting of the abnormal immune regulation underlying autoimmune conditions. We will report the results of a new study whereby we show that the preparatory regimen for HSCT is associated with a proportional expansion of cell with regulatory activity (T_{regs} and natural killer T cells). The induction of tolerance to the putative antigen is strictly dependent on the expansion of this network.The identification of professional and non-professional immunosuppressive cells and their biological properties is generating a huge interest for their clinical exploitation. More recently, mesenchymal stem cells (MSC) of bone marrow origin have been shown to exert a potent anti-proliferative effect which results in the inhibition of immune responses. Such an effect is not cognate dependent because it can still be observed using MSC from third-party donors fully mismatched for the MHC haplotype of the responder T cells or MSC which are constitutively negative for MHC molecules expression. Not only is MSC-induced unresponsiveness not antigen-specific, it also lacks of any selectivity. In fact, MSC are equally effective at inhibiting proliferation of memory and naïve T cells, do not preferentially affect CD4+ or CD8+ subsets and have similar effects IL-2-induced proliferation of natural killer (NK) cells. The mechanisms by which MSC induce immune tolerance is not confined by a direct action on the cells effecting immunity but also involve the recruitment of regulatory networks. Whilst MSC expand and activate regulatory T cells, they also have the capacity to interfere with the maturation and function of antigen presenting cells. The interaction between MSC and haemopoietic stroma is reciprocal because MSC depend on the presence of inflammatory molecules produced by monocytes/macrophages to become immunosuppressive. These properties have been extensively tested in animal models and in the clinical setting. It appears that the infusion of MSC have dramatic effects on a variety of auto- and allo-immune diseases. Most importantly, in the clinical setting MSC have been shown to improve conditions like graft rejection, aplastic anaemia, and severe steroid refractory graft-versus-host disease (GvHD). The mechanisms of their therapeutic effects remain to be fully elucidated but they involve a number of synergistic molecules that will be discussed in the context of innate tolerance.

Isolation and Localization of Stem Cells Nich in the Bulge of Human Hair Follicle

A B Mohd Hilmi[*], A S Halim[*], Z Idris[**], H Asma[***], E Nancy[****], T Stephan[****], P Ralf[****]

[*]Reconstructive Sciences Unit; [**]Department of Neurosciences, [***]Department of Anatomy; Universiti Sains Malaysia, Department of Dermatology, University of Lübeck, Germany

SUMMARY

Isolation of hair follicle stem cells (HFSC) was performed by plucking out the epithelial cores of full-length hair follicle before culturing in defined culture media. The primary culture proliferate and after one week the morphology of cells can be seen as small round, spindle and large flat cells. Localization of K15-GFP positive cells in human adult HF from scalp can be intravitally visualized *in situ* by non-viral transfection.

INTRODUCTION

The hair follicle is responsible for the production and growth of a hair[1]. It has three segments including the infundibulum which extends from the surface of the follicle to its sebaceous gland, isthmus which is consisted arrector pili muscle and inferior region to form hair bulb. Every single hair follicle comprises of epithelial and mesenchymal component. The epithelial hair follicle consists of the inner root sheath, the outer root sheath, hair matrix and hair shaft derive from epithelial stem cells in the bulge. The bulge involved in the generation of the new hair and supporting the microenvironment in which stem cells are found which is referred as stem cells niche. The mesenchymal hair follicle consists of the vascularized loose connective tissue called dermal papilla. Apart from mesenchymal and epithelial stem cells, the hair follicle also accommodates neural stem cells, melonocytes and smooth muscle cells lineages[2]. The multipotent stem cells make the hair follicle an enchanting organ for autologous source of stem cells and show a promising therapeutic for tissue engineering and tissue replacement therapy. This paper presents the isolation and localization of stem cells niche in the bulge of human hair follicle.

MATERIALS AND METHODS

Seven scalp samples from patients undergoing facelift surgery at München Clinic, Germany and Neurosciences Department at Hospital Universiti Sains Malaysia have been obtained for dissection. Scalp specimens were obtained from patients aged between 46 to 64 years old with informed consent. Within 24 hours after surgery, the scalp was washed to remove fat, cell debris and coated blood. The stem cells derived hair follicles (HFSC) were cultured with density at 1 x 10^4 cells per well in 24-well coated plate in a humidified atmosphere at 37 °C with 5% CO_2 incubator. For transient transfection of HF, K15-green fluorescent protein (GFP) construct were treated with Lipofectamin and incubated for four hours. The medium was change to fresh media before observation GFP positive signals *via* fluorescent microscope.

RESULTS

Stem cells from the harvested specimen were isolated and after analyzing by Cell Viability Analyzer, the cells have about 12.78 microns in diameter, the average circularity of cells is 0.92 out of 1.0 and more than 91.4 percent viability. The primary cells showed different type of cells can be distinguished as stem cells or progenitor cells are small round, the hair shafts are spindle and the transit - amplifying cells are becoming large flat cells after entering the route of terminal differentiation (Figure 1). Freshly isolated and transfected HF showed K15-GFP green expression in the bulge region (Figure 2).

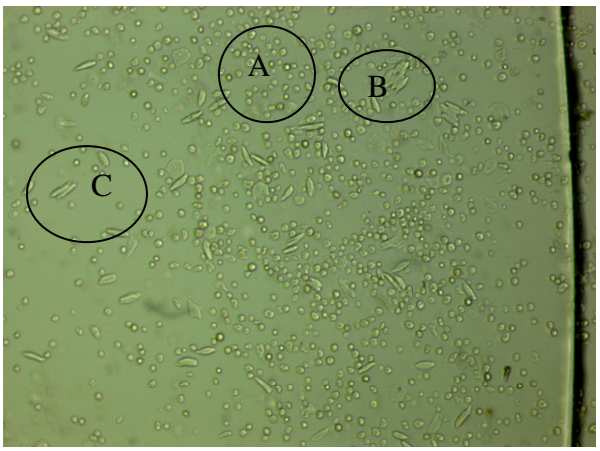

Fig 1: Primary culture consisting stem cells (A), transit amplifying cells (B) and hair shaft (C)

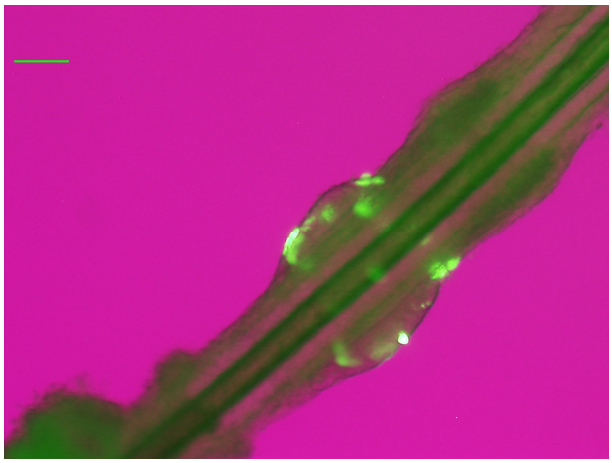

Fig 2: K15-GFP positive cells 40X

DISCUSSION

The human hair bulge is a stem cells niche and can be localized by Keratin 15 (K15) promoter both in situ and *in vitro*[3]. The demarcation and isolation can be transfected by non-viral means using K15 gene-promoter driven GFP labeling. The isolation and demarcation of K15 positive cells derived from human bulge is important for basic research to assess the ability of proliferation, characterisation and differentiation potential, thus serving as a new tool for cell-based regenerative medicine. K15-GFP positivity suggests that stem cells are located in the bulge.

REFERENCES

1. Ross MH, Kaye GI, Pawlina W. Histology A Text and Atlas Fourth Edition. Lippincott Williams & Wilkins. 2002
2. Yu H, Fang D, Kumar SM *et al.* Isolation of a novel population of multipotent adult stem cells from human hair follicles. *Am J Pathol* . 2006; 168:1879–1888
3. Stephen T, Norbert K, Jennifer EK *et al.* Nonviral In Situ Green Fluorescent Protein Labeling and Culture of Primary, Adult Human Hair Follicle Epithelial Progenitor Cells. *Stem cells.* 2009; 11:2793-803

Formation of Embryoid Bodies Comprising Three Embryonic Germ Layers from Rat Full-Term Amniotic Fluid-Derived Stem (AFS) Cells

F Nurfarhana[*], L Y Gao*, N Y Mohd[**], N Nordin**

[*]Stem Cell Research Laboratory, [**]Department of Obstetrics and Gynaecology, Faculty of Medicine and Health Sciences, Universiti Putra Malaysia (UPM) 43400 Serdang

SUMMARY

A subpopulation of cells expressing the stem cell factor receptor, c-Kit, and a marker for pluripotency, Oct-4, have been isolated from rat full-term amniotic fluid (AF), indicating that rat full-term amniotic fluid-derived stem (AFS) cells have been established. We have demonstrated for the first time, the formation of embryoid bodies (EBs) from rat full-term AFS cells, which strongly suggest their ability to differentiate into cells derivatives of the three primary germ layers. Prolonged culture of EBs show the formation of cells of different lineages, such as neurons (ectoderm), adipocytes (mesoderm) and endodermal cells (endoderm), based on their phenotypic changes, RNA analysis and protein analysis. These findings demonstrate that full-term AF serves as an excellent source of AFS cells, in mammals, including human. Hence, giving hopes that full-term AFS cells would be the future alternative source for stem cell therapy**.**

INTRODUCTION

AFS cells have been first discovered from mid-term AF in 2007 by a group of researchers in Wakeforest University, USA. They are pluripotent and represent only less than 1% in AF, thus isolation step is required in enriching these cells [1]. Formation of multi-cellular aggregates, EBs, *in vitro* is one of the characteristic of pluripotency, as they resemble the normal embryos of egg cylinder stage [2.] The endodermal layer of EBs is similar to embryo's primitive endoderm and the inner ectodermal layer of EBs is similar to embryo's primitive ectoderm [3.] EBs consist of differentiated cells of the three primary germ layers such as neurons, cardiomyocytes and hepatocytes [4.] The aim of this study is to characterize the pluripotency of full-term AFS cells by spontaneous differentiation through the formation of embryoid bodies (EBs).

MATERIALS AND METHODS

c-Kit positive cells were enriched from AF cell population using miniMACS (Miltenyi Biotec) , cultured in ES media in a gelatin-coated flask and subcultured by mild trypsinization. The same medium was used for c-Kit negative cells but without gelatin.EBs were induced by spontaneous differentiation, using hanging drop method [5]. The c-Kit positive cells were washed twice with 1x PBS and detached by trypsinization. Cell count was performed to get 4000 cells in every 20µl drops. Then, each drop was placed on the lid of petri dish to prevent their adherence to the plate and incubated in CO2 incubator for 4 days. On day four, the drops were transferred on a 48-well plate coated with 0.1% gelatin, using Pasteur pipette. The EBs were viewed under phase-contrast inverted microscope and the medium was changed every 3 days.

RESULTS AND DISCUSSION

Four samples of rat c-Kit positive cells from full-term AF samples were successfully cultured (Figure 1).

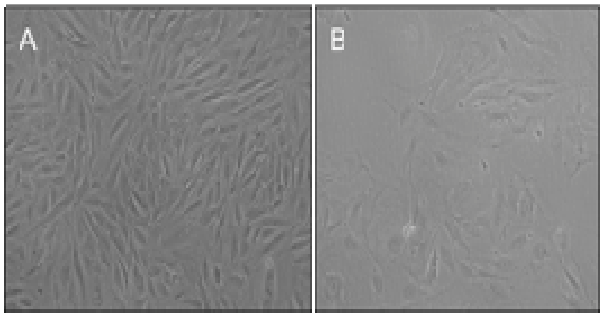

Fig1. Morphology of rat AF cells after immunoselection of c-Kit. No obvious difference was observed in the morphology of c-Kit positive cells (A) and c-Kit negative cells (B). The magnification is 10x.

Spontaneous differentiation was performed to induce the formation of EBs. Upon prolonged culture of the attached EBs, generation of cells phenotypically resemble the derivatives of the three primary germ layers were observed (Figure 2).

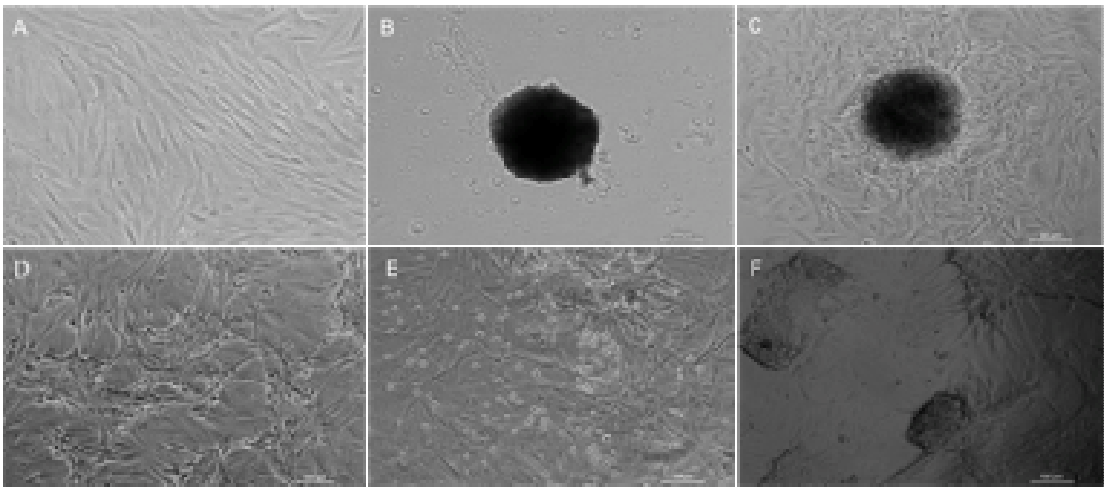

Fig2. Formation of embryoid bodies (EB) and differentiated cells from rat c-Kit positive cells. Rat c-Kit positive cells show more of fibroblast- and epithelial- like morphology (A). An EB of rat c-Kit positive cells on day 4 shows a solid round shape (B) and on day 7, the EB started to grow and expand (C). Prolonged culture of EBs result in formation of cells derivatives of the three primary germ layers; such as neuron-like cells (ectodermal lineage; D) adipocyte-like cells (mesodermal lineage; E) and endodermal-like cells (endodermal lineage; F). The magnification is 10x.

The ability of AFS cells or c-Kit positive cells to differentiate through the formation of EBs indicate that these cells may contain a population of cells with high potency

REFERENCES

1. De Coppi, P., Bartsch, G. Jr., Siddiqui, M.M, Xu, T., Santos, C.C., Perin, L., Mostoslavsky, G., Serre, A.C., Snyder, E.Y., Yoo, J.J., Furth, M.E., Sooker, S. and Atala, A. 2007. Isolation of amniotic stem cell lines with potential for therapy. *Nat. Biotechnol.* 25:100-106.
2. Doetschman, T.C., Eistetter, H., Katz, M., Schmit, W. and Kemler, R. 1985. The in vitro development of blastocyst-derived embryonic stem cell lines: formation of visceral yolk sac, blood islands and myocardium. *J. Embryol .Exp. Morphol.* 87:27-45.
3. Shen, M.M. and Leder, P. 1992. Leukemia inhibitory factor is expressed by the preimplantation uterus and selectively blocks primitive ectoderm formation in vitro. *Proc. Natl. Acad. Sci. USA*. 89:8240-8244.
4. Chinzei, R., Tanaka, Y., Shimizu-Saito, K., Hara Y., Kakinuma, S., Watanabe, M., Teramoto, K., Arii, S., Takase, K., Sato, C., Terada, N. and Teraoka, H. 2002. Embryoid-body cells derived from a mouse embryonic stem cell line show differentiation into functional hepatocytes. *Hepatology* 36:22-29.
5. Valli, A., Rosner, M., Fuchs, C., Siegel, N., Bishop, C.E., Dolznig, H., Madel, U., Feichtinger, W., Atala, A. and Hengstschlager, M. 2009. Embryoid body formation of human amniotic fluid stem cells depends on mTOR. *Oncogene* 29(7):966-977.

Mesenchymal Stem Cells-microglia Interactions in Response to Lipopolysaccharide

Z Rahmat, Y Y Ooi, R Ramasamy, S Vidyadaran*

Immunology Unit, Department of Pathology, Faculty of Medicine and Health Sciences, Universiti Putra Malaysia, Malaysia

SUMMARY

Multipotent mesenchymal stem cells (MSC) have been reported to have immunomodulatory effects on several immune cells. Our research tests the ability of MSC to regulate LPS-activated BV2 microglia cells. We found that MSC dynamically regulate nitric oxide production of BV2 based on BV2:MSC ratios of 1:0.2, 1:0.1, 1:0.02 and 1:0.01. BV2 proliferation was also inhibited in the higher co-culture ratio. Expression of the microglial activation marker CD40 was modulated by MSC in a dose-dependent manner. Secretion levels of IL-6, MCP-1, IL-10 and TNF-α were also modulated in co-cultures.

INTRODUCTION

Microglia are macrophages that reside in the central nervous system (CNS). They patrol the CNS and take on an activated phenotype when there is injury or stress (Hanisch and Kettenmann, 2007). Activated microglia elicit an inflammatory response, transforming from ramified to amoeboidal morphology, migrating towards the area of damage and secreting inflammatory mediators. The ensuing inflammation can be beneficial as it is capable of eliminating the disease agent. However constant activation of microglia in the CNS can be counterproductive resulting in neuronal damage and death, as suggested in neurodegenerative diseases including Parkinson's disease, stroke and Alzheimer's disease. Various approaches are being pursued to manage the chronic inflammatory responses of microglia. Mesenchymal stem cells (MSC) are highly mitotic cells with the capacity for self-renewal and differentiation. Studies have also found MSC to regulate immune responses by T-cells, B-cells, dendritic cells (DC) and natural killer cells (NK) (Ramasamy et al., 2008; Uccelli et al., 2007). This study aimed to investigate possible regulatory functions of MSC on microglia.

METHODOLOGY

MSC were isolated from ICR and Balb/c mice bone marrow. MSC were co-cultured with the BV2 immortalised microglia cell line at ratios 1:5, 1:10, 1:50 and 1:100. BV2 was activated with 1µg/ml lipopolysaccharide (LPS). Co-cultures were then assayed for nitric oxide with the Griess assay, proliferation by ^{3}H-thymidine incorporation assay, CD40 expression by immunophenotyping and cytokine expression with the BD Cytometric Bead Array Mouse Inflammation Kit assay.

RESULTS

Nitric oxide modulation by MSC.Following an LPS stimulation, BV2 cells produced up to 39.9 ± 0.7µM NO at 72 hours. In co-cultures, NO production was decreased in low ratio co-cultures (1:50 and 1:100) by up to 11.9µM ($p<0.05$) at 72 hours. Meanwhile, high ratio co-cultures increased the production of NO. This pleitropic effect suggests a dynamic role for MSC in modulating NO production. Cell-cell contact was found to be crucial for the surging levels of NO in high ratio co-cultures but not for the NO-reducing effects in low ratio co-cultures. MSC alone failed to produce NO in the presence of LPS at any of the ratios tested. However, transferring culture medium of LPS-activated BV2 cells to MSC cultures resulted in MSC producing high levels of NO (up to 31.2µM, $p<0.05$) following 96h culture with 48h of activated BV2 supernatant. ^{3}H-thymidine incorporation assay. Proliferation of BV2 cells was determined by using the ^{3}H-thymidine incorporation assay. MSC decreased proliferation of resting and LPS-activated BV2 cells in a dose-dependent pattern (up to approximately 50% in the highest BV2:MSC ratio (1:0.2; $p<0.05$). Preliminary results also show that soluble factors from both resting and LPS-activated BV2 cells decrease MSC proliferation by 23.8% and 44.4% respectively (Fig 1). Interestingly, we also show that addition of LPS alone is capable of increasing MSC proliferation (up to 62.8%; Fig 1).

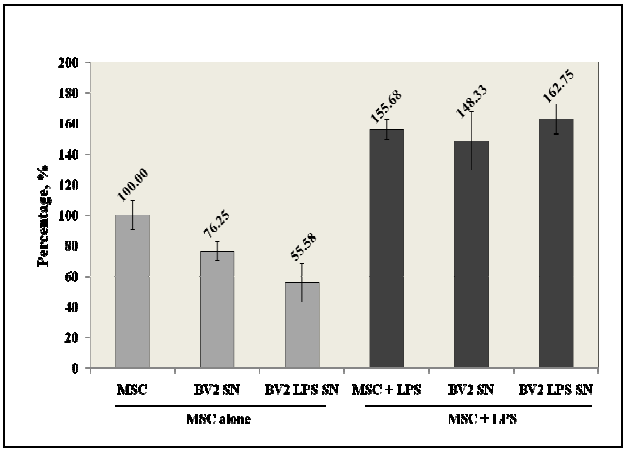

Fig 1. MSC proliferates after addition of LPS. MSC proliferation was determined 48 hrs after addition of resting and activated BV2 supernatant. Bar charts show proliferation of MSC with different treatments as indicated below the chart. Results are expressed in mean ± SD of triplicate wells in a 96-well plate and are representative of one independent experiment.

CD40 is a co-stimulatory molecule involved in microglia activation. Activating BV2 with LPS increased CD40 expression up to 87.8%. The three high ratios (1:0.2, 1:0.1 and 1:0.02) of BV2:MSC significantly limited expression of CD40 in a dose-dependent manner. CD40 expression of resting BV2 cells in co-cultures were reduced up to 52.2% compared to LPS-activated co-cultures that were reduced down to 28.2%. In transwell experiments, the two high ratios of co-cultures (1:0.2 and 1:0.1) inhibited CD40 expression of both untreated and LPS-treated BV2 cells.We used the BD™ Cytometric Bead Array assay to detect expression of IL-6, IL-10, MCP-1, IFN-γ, TNF-α and IL-12p70 cytokines in co-culture supernatants. We found that IL-6, MCP-1 and IL-10 cytokines production were increased (up to 6000pg/ml, 12000pg/ml and 70pg/ml respectively; Fig 2) in high ratios of BV2:MSC (1:0.2 and 1:0.1). Meanwhile, TNF-α production was decreased in co-cultures at all ratios, up to 500pg/ml at ratio 1:0.2 after 48h.

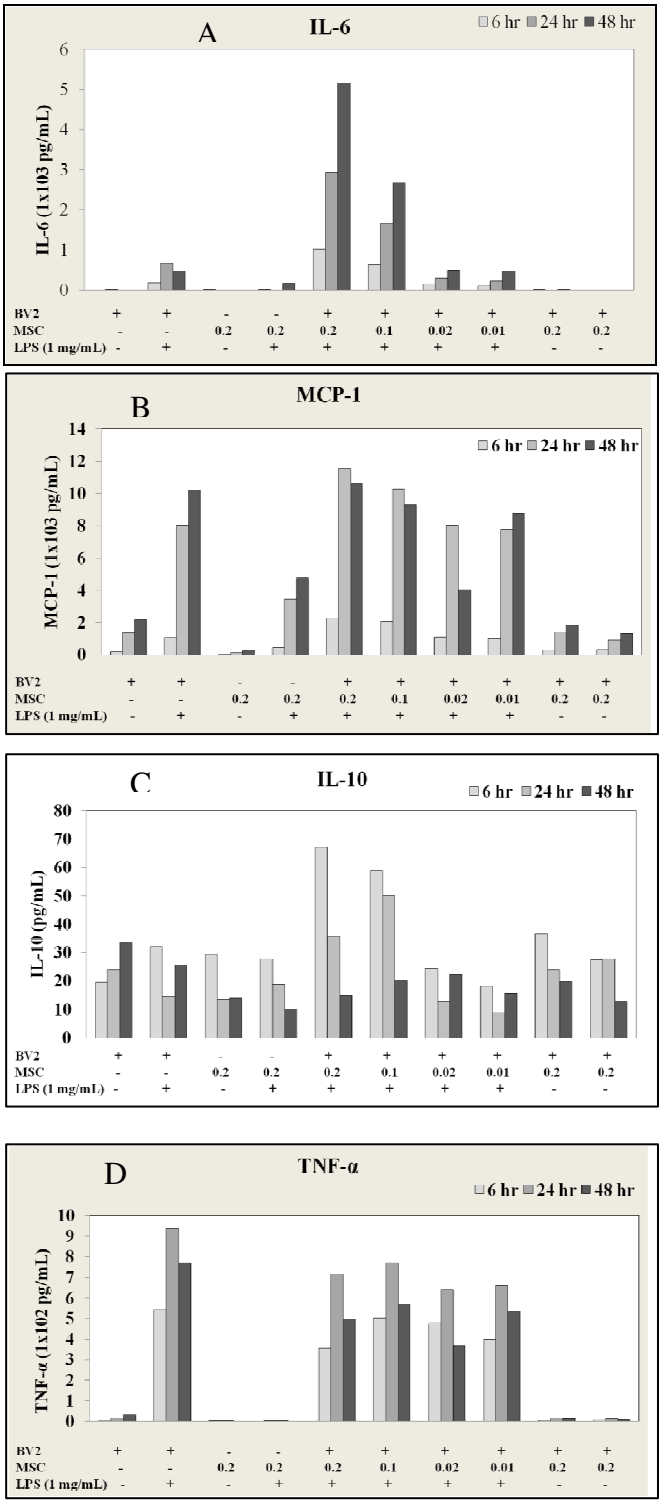

Fig 2. Cytokine production in BV2/MSC co-cultures. Production of IL-6, MCP-1, IL-10 and TNF-α (A, B, C and D respectively) were determined at 6, 24 and 48 hrs LPS stimulation. Bar charts show cytokine production after co-culture with different treatment as

indicated below charts. Results are representative of one independent experiment.

DISCUSSION

The results show MSC to be capable of regulating inflammatory responses of microglia. The effect of MSC on NO production in microglia co-cultures is dependent on the number of MSC. We also show that activated microglia produce soluble factors that stimulate MSC to produce NO. MSC also decreases proliferation of microglia and reduces expression of the microglial activation marker CD40, particularly in resting cells. Expression of cytokines involved in inflammation is also affected, and warrants further investigation.

REFERENCES

1. Hanisch, U.K., and Kettenmann, H. (2007). Microglia: active sensor and versatile effector cells in the normal and pathologic brain. Nat Neurosci *10*, 1387-1394.
2. Ramasamy, R., Tong, C.K., Seow, H.F., Vidyadaran, S., and Dazzi, F. (2008). The immunosuppressive effects of human bone marrow-derived mesenchymal stem cells target T cell proliferation but not its effector function. Cell Immunol *251*, 131-136.
3. Uccelli, A., Frassoni, F., and Mancardi, G. (2007). Stem cells for multiple sclerosis: promises and reality. Regen Med *2*, 7-9.

Human Umbilical Cord Derived Mesenchymal Stem cells Suppress T Cell Proliferation Through Cell Cycle Arrest

C K Tong[*], B C Tan[**],H F Seow[*] , R Ramasamy[*]

[*]Department of Pathology, Faculty of Medicine and Health Sciences, University Putra Malaysia, [**]Britannia Women & Children Specialist Centre, Kajang, Selangor, Malaysia

SUMMARY

The immunomodulatory activity of mesenchymal stem cell (MSC) promises a great therapeutic potential in cell-based therapy to treat various immunological disorder such as graft versus host disease and autoimmune diseases. In this study, we have identified and generated a MSC-like population from human umbilical cord tissues, termed as human umbilical cord mesenchymal stem cell (UC-MSC) and explored its immunomodulatory properties. Using appropriate co-culture systems, the effects of UC-MSC on rested or activated T cell proliferation, activation markers expression and cell cycle status were elucidated.

INTRODUCTION

International Society for Cellular Therapy working group has defined adult MSC as plastic adherent cells; express a panel of specific surface markers (e.g., CD14-, CD34-, CD45- and MHC class II-and CD73+, CD29+, CD105+); capable of self-renewal and differentiating into multiple mesenchymal lineages (1). We have previously shown that, MSC from bone marrow origin exert an immunomodulatory effect on T, B and dendritic cell population via cell cycle arrest (2-4). In this study, we have explored the potential of umbilical cord derived MSC on exerting a similar Immunosuppression on T cells.

Fig 1. UC-MSC inhibit stimulated T cell proliferation in dose dependent manner.

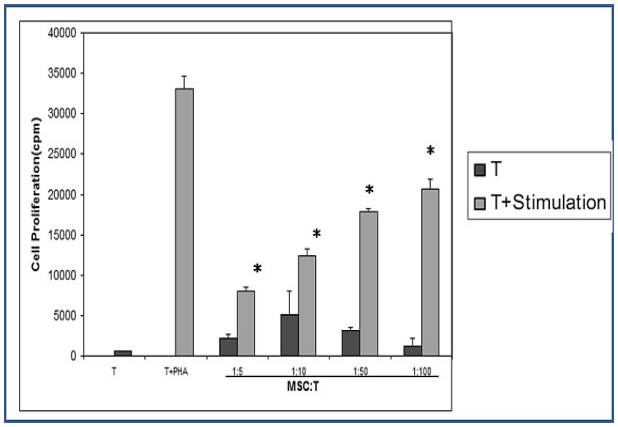

MATERIALS AND METHODS

UC-MSCs were generated from human umbilical cord using enzymatic-mechanical dissociation method. Human PBMC (peripheral blood mononuclear cells) were isolated from normal human peripheral blood sample using density gradient separation method. T cell proliferation was measured using ^{3}H-TdR incorporation assay after co-culture with resting or PHA-L/ anti -CD3/CD28 micro beads stimulation for 72 hours. T cell activation was accessed by evaluating CD25 and CD69 surface markers expression of resting and stimulated T cell after co-cultured with UC-MSC at 1: 10 ratio (UC-MSC:T) using flow cytometry. Cell cycle analysis was performed using propidium iodine (PI) and fluorescein isothiocyanate (FITC) co-staining to determine DNA content and intracellular protein, respectively.

RESULTS

Fig 2. UC-MSC do not prevent priming of T cells

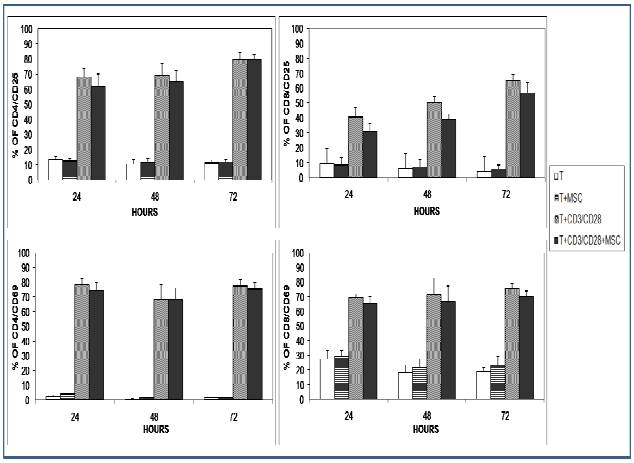

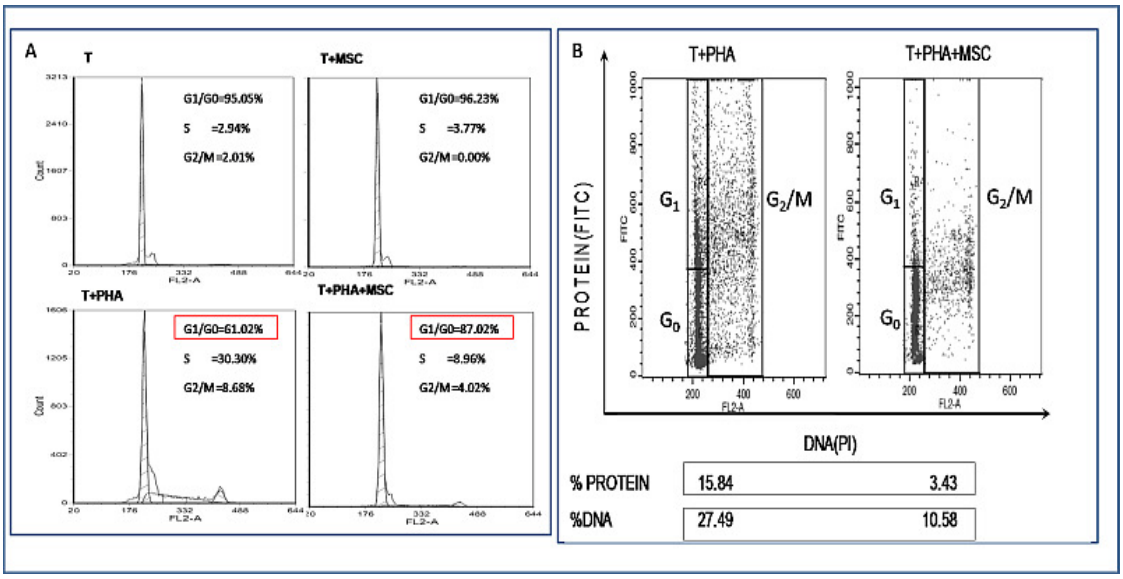

Fig 3. (A) UC-MSC arrest activated T cell in G0/G1 phase of cell cycle. (B) UC-MSC profoundly inhibit both protein and DNA synthesis of activated T cell.

DISCUSSION

Our data indicated that UC-MSC suppress T cell proliferation triggered by PHA-L or anti-CD3/CD28 micro beads in dose dependent manner (Figure.1). This inhibitory effect does not affect the T cell priming (Figure 2) however it arrests the T cells in anergy status by blocking both protein and DNA synthesis (Figure 3). The results show that UC-MSC exert an anti-proliferative effect on T cells by prevent them to enter into cell cycle thus maintain at quiescent state in G0 phase.

REFERENCES

1. Dominici M, Le Blanc K, Mueller I, Slaper-Cortenbach I, Marini F, Krause D, et al. Minimal criteria for defining multipotent mesenchymal stromal cells. The International Society for Cellular Therapy position statement. Cytotherapy. 2006;8(4):315-7.
2. Tse WT, Pendleton JD, Beyer WM, Egalka MC, Guinan EC. Suppression of allogeneic T-cell proliferation by human marrow stromal cells: implications in transplantation. Transplantation. 2003 Feb 15;75(3):389-97.
3. Najar M, Rouas R, Raicevic G, Boufker HI, Lewalle P, Meuleman N, et al. Mesenchymal stromal cells promote or suppress the proliferation of T lymphocytes from cord blood and peripheral blood: the importance
4. of low cell ratio and role of interleukin-6. Cytotherapy. 2009;11(5):570-83.
5. Ramasamy R, Tong CK, Seow HF, Vidyadaran S, Dazzi F. The immunosuppressive effects of human bone marrow-derived mesenchymal stem cells target T cell proliferation but not its effector function. Cell Immunol. 2008 Feb;251(2):131-6.

Manganese Doping on Biphasic Calcium Phosphate Ceramics for Machanical Improvement

I Sopyan

Department of Manufacturing and Materials Engineering, Kulliyyah of Engineering, International Islamic University, Kuala Lumpur 50728, Malaysia

SUMMARY

Manganese doped biphasic calcium phosphate powders have been synthesized via sol-gel method. The powders are of nanosize and high crystallinity. Dense pure BCP and Mn-doped BCP ceramics were fabricated via uniaxial pressing using the sol-gel derived powders. The compacted discs were sintered in air atmosphere with temperatures ranging from 1000 ºC to 1400 ºC. The presence of manganese improves the densification in the BCP mixture as the relative density increased with Mn doping and also sintering temperature. Considerable grain growth has been observed at 1300 ºC for Mn-doped BCP samples compared to the pure BCP. Furthermore, 15 mol% Mn showed the maximum hardness value of 6.66 GPa at 1400 ºC compared to pure BCP of only 2.89 GPa. Similarly, the Mn-doped BCP has superior fracture toughness where it attained maximum values of 1.05 $MPam^{1/2}$ at 1400 ºC compared to 0.72 $MPam^{1/2}$ at 1300 ºC of pure BCP.

INTRODUCTION

Hydroxyapatite (HA) have been long applied for a bone implant material due to its excellent bioactivity to living hard tissues. Its brittleness, however, have been a big mechanical concern when applied for load bearing bone implant. Various studies have been carried out to improve the mechanical properties of sintered HA. It is important to note that, dense HA has a compressive strength four times that of cortical bone, but yet it shows a significantly lower tensile strength and fracture toughness. One of promising approaches that have been used to improve the mechanical performance of HA is by doping with different sintering additives such as metal ions[1,2]. Dense BCP compacts have been prepared via uniaxial pressing followed by pressureless sintering[1,3,4]. Inclusion of Mn in BCP has not been studied extensively although numerous works have reported the significant role of manganese oxide in promoting densification in other ceramics systems[5]. In this study, the effects of Mn doping and sintering temperature on mechanical properties of the dense BCP ceramics were studied.

MATERIALS AND METHODS

Sol-gel derived pure BCP and Mn-doped BCP powders[6], with four different molar concentrations (0.01 mol%, 2 mol%, 5 mol% and 15 mol%) have been chosen for compaction. In the selection, 5 mol% Mn-doped BCP was purposely chosen as this powder contained the highest amount of β-TCP among all the synthesized Mn doped BCP powder. The powders were uniaxially compacted at 2.5 MPa pressure into disc shapes (20 mm diameter x 5 mm thickness) using a hardened steel mould and die set. For each powder concentration, 7 samples were fabricated. In this research study, the sintering approach adopted was the conventional pressureless sintering. The green bodies were sintered in air using a heating furnace (Protherm, PLF 160/5,) at seven different temperatures ranging from 800-1400 °C and firing for 2 hours. The ramp-rate was fixed at 2°C/min for both heating and cooling process).

RESULTS AND DISCUSSION

Fig. 1 presents TGA curves of Mn-doped BCP powders. It was revealed that as Mn content increases, the crystallization and decomposition to biphasic mixtures occurred at a lower temperature. The figure also shows the starting temperature for crystallization of HA and the decomposition temperature of pyrophosphate to biphasic mixtures of pure BCP and Mn-doped BCP. The result reveals that doping of Mn up to 15 mol% has reduced the crystallization temperature of HA and formation temperature of biphasic mixtures. From the 15 mol% Mn-doped BCP plot, it can be seen that the HA crystallization and TCP formation have occurred at the temperature of about 381 ºC and 704 ºC, respectively. In fact, the 15 mol% Mn-doped BCP shows the lowest temperatures for both the HA crystallization and TCP formation among all the Mn-doped BCP samples. Therefore, it can be inferred that Mn acts as calcination additive to the BCP.

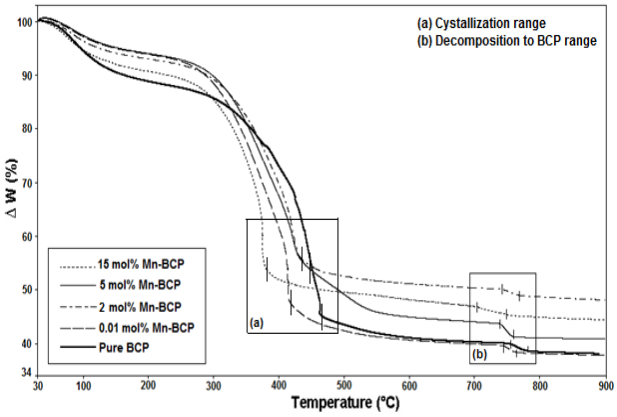

Fig. 1: TG/DTA of black gel of pure BCP and Mn-doped BCP

After compacted and sintered at various temperatures, the produced dense bodies are subjected to X-ray diffraction (XRD) analysis. All dense compacts produced peaks of HA phase that correspond to the standard ICDD card no: 09-432 for HA with no secondary phases such as α-TCP, TTCP or CaO being detected. From the effect of sintering temperature on the relative density results, it was deduced that the increase in relative density was irrespective of Mn content. This was due to the observation for pure BCP dense samples whereby the relative density also increased with increase in sintering temperature though without Mn doping as summarized in Table 1. Generally, the density variation of all the composition studied exhibited a similar trend with increasing sintering temperature. All the samples attained above 82 % of theoretical density at all temperatures. However, the undoped BCP could only achieve the highest value of 91 % at 1300 ºC, which could be achieved by 5 mol% Mn-doped BCP at lower temperature of 1200 ºC. However, it still shows a pronounce increase in density with temperature increase. For 1 mol% Mn and 2 mol% Mn, the maximum densification of 92 % and 93%, respectively, was attained at 1300 ºC. Meanwhile, 15 mol% Mn only attained the highest of 98 % relative density when sintered at 1400 ºC as compared to 5 mol% Mn which attained 99% densification at 1300ºC and 1400 ºC. However, other research on dense pure HA found that sintering above 1300 ºC was required to achieve 98% of theoretical density[7,8]. This difference in finding could be related to the difference in powder characteristics used.

Sintering Temperature (ºC)	Pure	0.01 mol% Mn	2 mol % Mn	5 mol% Mn	15 mol% Mn
800	80	82	85	87	89
900	82	83	86	88	89
1000	86	86	88	89	90
1100	87	88	89	91	90
1200	90	90	91	92	93
1300	91	92	93	99	96
1400	90	91	92	99	98

Table 1. Relative density of BCP dense samples at various sintering temperatures

Meanwhile, in the study of effect of Mn content on the relative density, it was observed that increase in doping of Mn content has improved the densification behaviour of the BCP (Table 1). It can be seen that sintering at 1000 ºC has resulted in massive improvement of densification for the BCP with Mn doping. The increase of relative density has increased greatly from 86 % to 88% with only 2 mol% of Mn doped into the BCP. The further increase to 89 % and 90 % were found for 5 mol% and 15 mol% of Mn doping, respectively. At 1300 ºC of sintering temperature, the densification was pronouncedly increased to 99% for 5 mol% Mn compared to 91 % and 92 % of relative density for pure and 2 mol% Mn-doped BCP. In this study, 5 mol% Mn-doped BCP exhibited the highest densification of 99 % at 1300ºC among all the samples. Thus, incorporation of Mn as sintering additive into BCP has improved its densification. This more progressive densification is presumably due to higher thermal stability of BCP phase as thermal stability of the starting allowed the samples attaining fully densification at high sintering temperature[9].

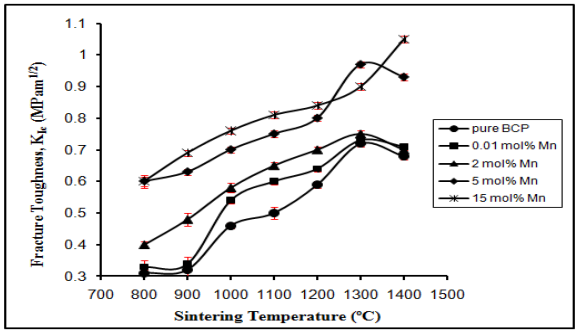

Fig. 2: Effect of sintering temperature and Mn doping on the fracture toughness of BCP

The effects of sintering temperature and Mn doping on the fracture toughness of the five BCP compacts are shown in Fig. 2. Similar trend of Vicker's hardness was observed for the fracture toughness, K_{Ic} that is the Mn doped BCP compacts showing better properties than the pure BCP compacts throughout the sintering regime. For the pure BCP sintered compacts, the K_{Ic} was observed to increased from the lowest value of 0.31 MPam$^{1/2}$ at 800 ºC to the maximum value of 0.72 MPam$^{1/2}$ at 1300 ºC, followed by decrement of the K_{Ic} value to 0.68 MPam$^{1/2}$ at 1400 ºC. Likewise, the fracture toughness of the Mn doped sintered samples of 0.01 mol%, 2 mol% and 5 mol% showed improvement in fracture toughness with sintering tempearture up to 1300 ºC followed by a sign of deterioration at 1300 ºC. The maximum values achieved at 1300 ºC are of 0.73 MPam$^{1/}$2, 0.75 MPam$^{1/2}$ and 0.97 MPam$^{1/2}$. As Mn content increased to 5 mol% and 15 mol%, pronounce improvement with similar trend was observed where both samples showed a sharp increased between 900 ºC and 1200 ºC and the maximum K_{Ic} achieved for 5 mol% Mn was 0.97 MPam$^{1/2}$ at 1300 ºC. Meanwhile, the K_{Ic} for 15 mol% Mn continuously increased to 1.05 MPam$^{1/2}$ at 1400 ºC which is dissimilar from the trend observed for pure BCP and the three other Mn-doped samples. This value was also the maximum value of K_{Ic} attained in this research work. Thus, it can be inferred that doping of Mn has greatly improved the fracture toughness of BCP.

CONCLUSION

Manganese doping though sol-gel method has improved the thermal stability of dense BCP up till 1400 ºC. Mn has acted as sintering additives for BCP such that HA phase stability was not disrupted by the fabrication of dense samples parameters such as the initial pressing conditions, sintering cycle and temperature employed. Presence of manganese improves the densification of the BCP mixture as the relative density increased with sintering temperature and Mn doping. The maximum relative density was achieved by 5 mol% Mn with 99 % at 1300 ºC. Furthermore, 15 mol% Mn showed the maximum hardness value of 6.66 GPa at 1400 ºC. Similarly, the Mn-doped BCP has superior fracture toughness than the pure BCP and increase in sintering temperature has improved the fracture toughness of both pure and Mn-doped BCP samples. Thus, it can be concluded that doping of Mn has greatly improved the hardness and fracture toughness of BCP.

REFERENCES

1. Gibson IR and Bonfield W. Preparation and characterization of magnesium/carbonate co-substituted hydroxyapatite. J. Mater. Sci. Mater. Med. 2002; 13: 685-93.
2. Lilley KJ, Gbureck U, Knowles JC, Farrar DF and Barralet J. Cement from magnesium substituted hydroxyapatite. J. Mater. Sci. Mater. Med. 2005; 16: 455-60.
3. Muralithran G and Ramesh S. The effects of sintering temperature on the properties of hydroxyapatite. Ceram. Int. 2000; 26: 221-30.
4. Jolata S, Tas AC and Bhaduri S. Microwave assisted synthesis of calcium phosphate nanowhiskers. J. Mater. Res. 2004; 19: 1876-81.
5. Ramesh S, Tan CY, Sopyan I, Hamdi M and Teng WD. Consolidation of nanocrystalline hydroxyapatite powder. Sci. Technol. Adv. Mater. 2007; 8: 124-30.
6. Sopyan I and Natasha AN. Preparation of nanostructured manganese doped biphasic calcium phosphate powders via sol-gel method. IONICS. 2009; 15:735-41.
7. Best S and Bonfield W. Processing behaviour of hydroxyapatite powders with contrasting morphology. J. Mater. Sci. Mater. Med. 1994; 5: 516-21.
8. Van Landuyt P, Li F, Keustermans JP, Streydio JM, Delannay F and Munting E. The influence of high sintering temperatures on the mechanical properties of hydroxyapatite. J. Mater. Sci. Mater. Med. 1995; 6: 8-13.
9. Ramay HR and Zhang M. Preparation of porous HA scaffolds by combination of the gel-casting and polymer sponge methods. Biomaterials. 2003; 24:3293-302.

Carbodiimide is a Better Cross Linking Agent for Sheep Tendon Collagen

M B Fauzi [*], M A Amri [*], S Aminuddin [*,], B H I Ruszymah [*,***]**

[*]Tissue Engineering Centre, UKM Medical Centre, Kuala Lumpur, alaysia,[**]Ampang Puteri Specialist Hospital, Kuala Lumpur, Malaysia,[***]Department of Physiology, Faculty of Medicine, UKM Malaysia

SUMMARY

Collagen sponge has great potential as scaffold in skin tissue engineering. Collagen was isolated from sheep tendon by freeze-dried technique. Collagen sponge was formed from the purified collagen powder and crosslinked with glutaraldehyde (GA) or carbodiimide (EDC). MTT (3-(4,5-dimethylthiazol-2-yl)-2,5-diphenyltetrazolium bromide) assay test and Alkaline Comet assay was evaluated towards human dermal fibroblast. The results indicate that, EDC-collagen sponge has less cytotoxic and genotoxic effect compared to GA-collagen sponge. Therefore EDC is a better crosslink agent for sheep tendon collagen.

INTRODUCTION

Collagen is one of the components in extracellular matrix secreted by dermal fibroblast that plays a major role in the design of skin structure. It consist of collagen type I and III [1]. The aim of biomaterial application in tissue engineering is as a scaffold to replace or improve tissue function [2]. Collagen scaffold is used as temporary scaffold to give support to the 3-dimensional tissue construct [3]. However, natural biomaterial has mechanical weakness but can still be modified by physical approach such as ultraviolet or chemical substance, such as carbodiimide (EDC) and glutaraldehyde (GA) [4]. This study evaluated the effect of two crosslink agent; GA and EDC toward sheep tendon collagen. Cytotoxicity and genotoxicity towards these agents were tested.

MATERIALS AND METHODS

Collagen was extracted from sheep tendon. Tendon was isolated from the sheep, dissolved in acetic acid and freeze-dried to obtain collagen powder. Collagen sponge was formed from the purified collagen powder and crosslinked with either EDC and GA. After the crosslink process, collagen sponges were irradiated by gamma irradiation for sterilization. The crosslinked-collagen sponge were prepared for the MTT (3-(4,5-dimethylthiazol-2-yl)-2,5-diphenyltetrazolium bromide) assay and Alkaline Comet assay. Both test were evaluated towards human dermal fibroblast. Irradiated non-crosslinked collagen sponges were used as control.

RESULTS

50% EDC-collagen leachate has the highest cell viability (89.6%) and 100% EDC-collagen showed 81% viability but it did not exceed 50% cell damage (I_c50) (Fig.1). Following this, only 100% EDC-collagen sponge was choosen for genotoxicity analysis by using Comet assay evaluation. Comet score evaluation of tail moment and % DNA in tail showed that 100% EDC-collagen sponge did not has genotoxic effect (Fig.2).

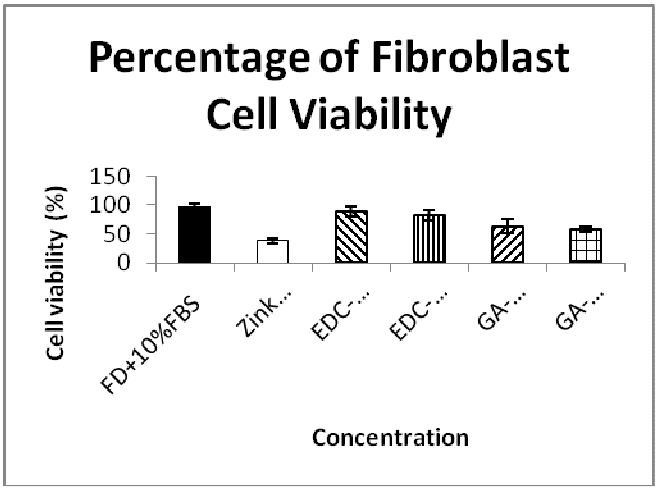

Fig.1: Percentage of human dermal fibroblast cell viability at different concentration of crosslinking agent. Zink Sulphate is the positive control, exhibiting cell viability of 41.5%. the lowest cell viability demonstrated is GA-collagen (100%) which is 56%. However, it still not exhibit cytotoxic effect.

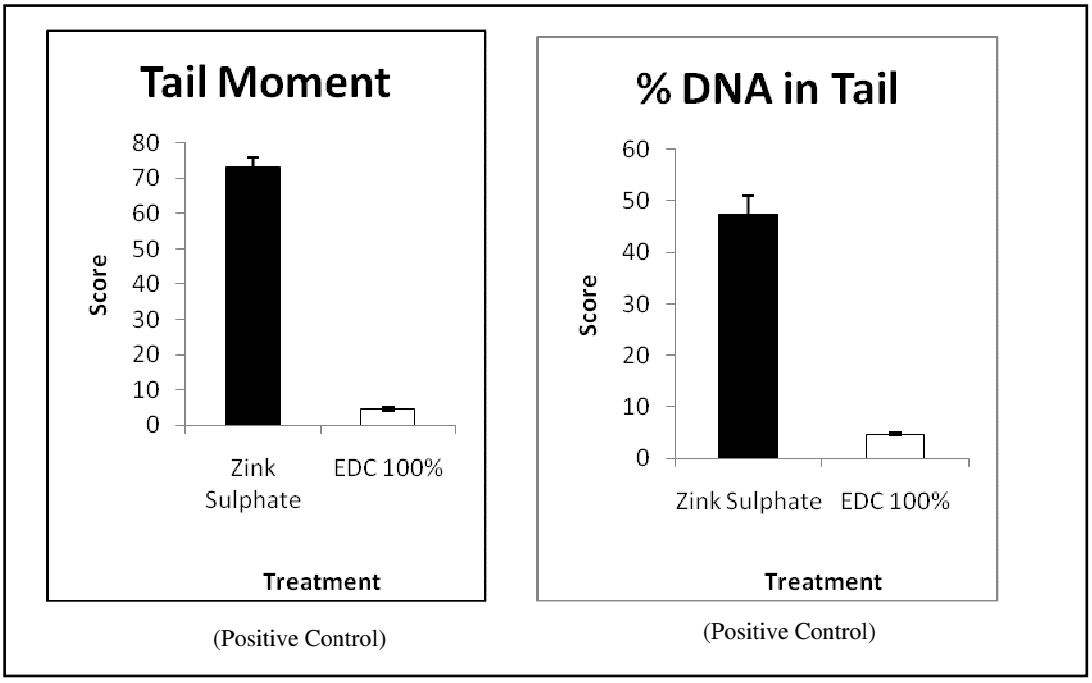

(Positive Control) (Positive Control)

Fig.2: Comet assay evaluation via Tail Moment & DNA in Tail. Tail moment of more than 60 and % DNA in tail of more than 5 is considered genotoxic. So, 100% EDC is not genotoxic.

* EDC-Collagen (100%) concentration versus $ZnSO_4$ ($p<0.05$)

DISCUSSION

Collagen sponge crosslinked with EDC demonstrated good biocompatibility properties toward human dermal fibroblast. Therefore, EDC is a better crosslinking agent compared to GA for sheep tendon collagen.

REFERENCES

1. Epstein, E.H.J. & Munderloh, N.H. Human skin collagen. Presence of type I and type III at all levels of the dermis. *J Biol Chem*. 1978;253: 1336-1337.
2. Filippo, R.E.D., Yoo, J.J. & Atala, A. Engineering of Vaginal Tissue *in vivo*. *Tissue Engineering*.2003;9(2): 301-306.
3. Ma, P.X. Scaffolds for tissue fabrication. *Materials Today.* 2004; 30-40.
4. Lee, H.C., Singla, A. & Lee, Y. Biomedical application of collagen. *International Journal of Pharmaceutic.* 2001;221: 1-22.

Optimization of Process Conditions for High Cell Density Proliferation of DF-1 Cells in Bioreactor

M Mel[*], M A Arifin[*], H N Sohif[*], SS Hassan[**]

[*]Department of Biotechnology Engineering, Kulliyah of Engineering, International Islamic University Malaysia, Gombak, P.O. Box 10, 50728 Kuala Lumpur, [**]School of Medicine and Health Sciences, Monash University, Jalan Lagoon Selatan, Bandar Sunway, 46150, Selangor.

SUMMARY

The purpose of this study was to optimize agitation speed, microcarrier concentration and pO_2 levels in bioreactor for culturing DF-1cells in DMEM media supplemented with 7% fetal bovine serum. Statistical analysis has shown that the model derived from the results was proven to be significant and pO_2 level turned out as the most significant parameter in the experiment. As predicted by analysis, cells grew up to 1.190×10^6 cells/ml when moderate agitation speed, microcarrier concentration, and pO_2 level are applied.

INTRODUCTION

DF-1 cells which was discovered by Douglas N. Foster is a spontaneously immortalized continuous cell line derived from chicken embryonic fibroblast, CEF [2]. The cell line is widely used in various researches as it has rapid cell proliferation and useful as substrates for virus propagation, recombinant protein expression and recombinant virus production [3]. The cell line is anchorage dependent thus it requires surface for attachment (e.g. microcarrier beads) when cultured in stirred tank bioreactor [1]. In this study, growth of DF-1 cells in bioreactor will be optimized by manipulating several process parameters.

MATERIALS AND METHODS

Dulbecco's Modification of Eagle's Medium (DMEM) supplemented with 7% fetal bovine serum was used to culture and maintain DF-1 cells. By using STATISTICA ® software, 3**(3-1) Fractional Factorial Design was generated and was used to assist the cell growth optimization study. Three parameters that were chosen to be manipulated in nine runs of experiment are agitation speed, Cytodex 1® microcarrier concentration, and pO_2 levels. Cultures were performed in a 1.5 L bioreactor (Infors HT, Switzerland) with one liter working volume and equipped with an elephant ear impeller. Cell inoculum density for all runs was 1×10^5 cells/ml.

RESULTS

Table 1 shows the result for each run of the experiment. Maximum cell concentration of 1.210×10^6 cells/ml was achieved at Run 5. Using statistical tool, a model is derived from the results. Analysis of variance (ANOVA) proved that the derived model is significant as the p value is lower than 0.05 and the most significant parameter in the experiment is pO_2 level.

Table 1. Maximum cell concentration obtained for each run

Run	Agitation speed (rpm)	Microcarrier concentration (g/l)	pO_2 (%)	Max cell concentration (cells/ml)
1	70	5	10	1.045×10^6
2	50	5	30	0.615×10^6
3	50	3	50	0.500×10^6
4	50	1	10	0.820×10^6
5	70	3	30	1.210×10^6
6	90	5	50	0.420×10^6
7	70	1	50	0.525×10^6
8	90	3	10	0.865×10^6
9	90	1	30	0.865×10^6

For predicting the optimal values of maximum cell concentration, a linear model was developed: Y (maximum cell concentration) = -2080694 + 79167 (A) - 560 (A^2) + 177500 (B) -30417 (B^2) + 23417 (C) - 573 (C^2); where cell concentration produced as yield (Y); stirrer speed (A); microcarrier concentration (B); and pO_2 (C). Correlation coefficient or R of the model is 0.95195 indicates high degree of correlation between experimental and predicted values.

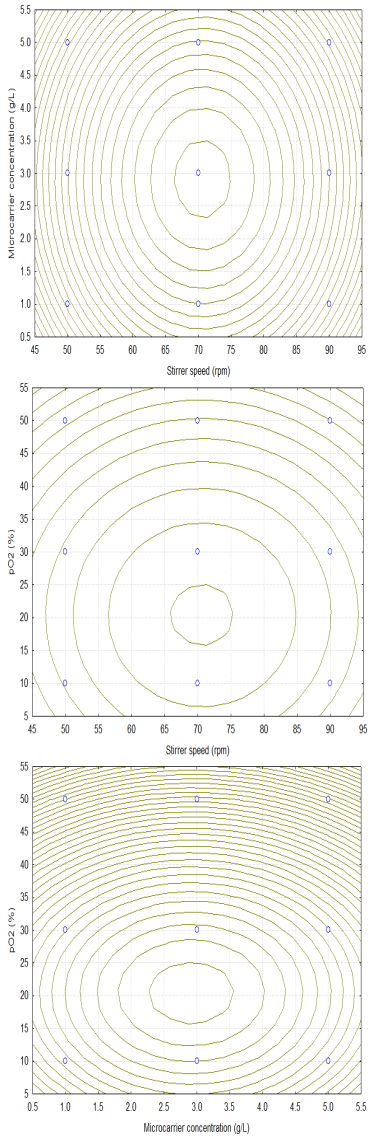

Fig 1. 2D contour plots show the effect of agitation speed, microcarrier concentration and pO_2 level on maximum cell concentration.

The linear model was validated in another experiment and maximum cell concentration of 1.190 x 10^6 cells/ml was achieved when agitation speed was 71 rpm, microcarrier concentration was 2.9 g/l and pO_2 was 20%.

DISCUSSION

Based on the results, DF-1 cells will have maximum concentration when moderate values of agitation speed, microcarrier concentration, and pO_2 level are applied. This condition is more suitable for the cells as they become more sensitive at higher hydrodynamic condition as reported by many researchers [4, 5.6]. In this case study, growth of DF-1 cells in bioreactor is most affected by pO_2 level followed by agitation speed and finally microcarrier concentration. PO_2 level has been proven to have a major role in the growth of cells in bioreactor.

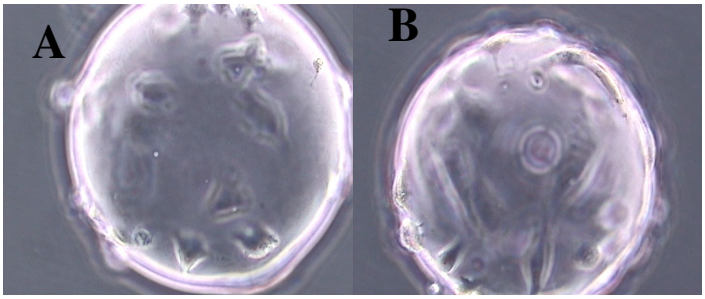

Fig 2. Attachment of DF-1 cells on Cytodex 1 microcarriers at different times. (A) 8 hours (B) 32 hours (C) 56 hours (D) 80 hours.

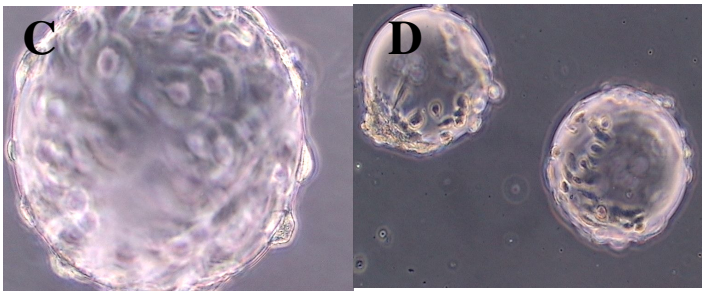

REFERENCES

1. Himly, M., Foster, D. N., Bottoli, I., Iacovoni, J. S. and Vogt, P. K. (1998). The DF-1 Chicken Fibroblast Cell Line: Transformation Induced by Diverse Oncogens and Cell Death Resulting from Infection by Avian Leucosis Virus. *Virology 248(2),* pp.295-304.
2. Kim, H., You, S., Kim, I. J., Farris, J., Foster, L. K., and Foster, D. N. (2001). Increased mitochondrial-encoded gene transcription in immortal DF-1 cells. *Exp Cell Res 265 (2),* pp.339-347.
3. Freshney, R. I. (2005). Culture of Animal Cells: A Manual of Basic Technique 5th Edition. New York: Wiley-Liss.
4. Arifin, M. A., Mel, M., Karim, M. I. A., and Aini, I. (2010). Production of Newcastle disease virus by Vero cells grown on Cytodex 1 microcarriers in a 2-Litre stirred tank bioreactor. *Journal of Biomedicine and Biotechnology vol. 2010.*
5. Maranga, A., Cunha, A., Clemente, J., Cruz, P., and Carrondo, M. J. T. (2004). Scale-up of virus-like particles production: effects of sparging,cagitation and bioreactor scale on cell growth, infection kineticscand productivity. *Journal of Biotechnology 107,* pp.55-64.
6. Frahm, B., Brod, H., and Langer, U. (2009). Improving bioreactor cultivation conditions for sensitive cell lines by dynamic membrane aeration. *Cytotechnology 59 (1),* pp.17-30.

Adaptation of U937 Cell in Agitation Culture

M I Fauzi*, F A Abdul Majid*

*Department of Bioprocess Engineering, Faculty of Chemical Engineering and Natural Sources, Universiti Teknologi Malaysia.

SUMMARY

This research is done to investigate the potential of Human Caucasian Lymphoma cell U937 to be grown in stirred tank bioreactor to produce high mass product of the cells.

INTRODUCTION

Cells and tissue culture technique are needed in order to supply enough cells to do the bioassay analysis and high-throughput screening. Some of the cells that usually used are Human Skin Fibroblast and Human Caucasian Lymphoma U937. Billions of cells are needed in high-throughput screening. To have the cell culture in t-flask method for this type of analysis is not practical. Culturing the cell inside bioreactor is more promising in order to maximize the production rate of the cell and minimize the number of manpower.

MATERIALS AND METHODS

Human Caucasian Histiocytic Lymphoma U937 cells are grown in RPMI 1640 medium. The cells were maintained at 37°C, 5% humidified CO_2 incubator. Initial seeding concentration of 2 x 10^5 cells/ml will be introduce into 1 L spinner flask with the total working volume of 100ml. The flask caps were loosening a bit to allow the gas transfer into the flask and placed in 37°C, 5% CO_2 incubator. The impeller speeds were varying from 20, 50 and 100 rpm. Cell growths were monitored every 24 hours by haemocytometer for viable cells count.

RESULTS

The growth profile for U937 cells in static culture and under agitation in spinner flask are plotted. The graphs were compared to see the best growth profile for U937 cells. The maximum cell concentration for static culture is 17 x 10^5 cells/ml. The highest cell concentration in 20, 50, and 80 rpm of agitation is 2.3 x 10^5 cells/ml, 7.2 x 10^5 cells/ml, and 2.5 x 10^5 cells/ml respectively.

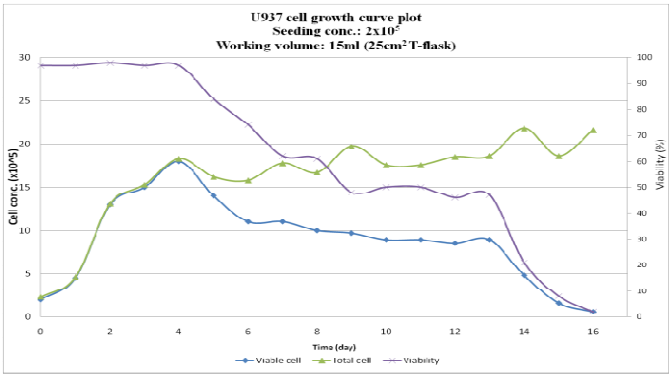

Fig 1 Growth profile for U937 cells in static culture

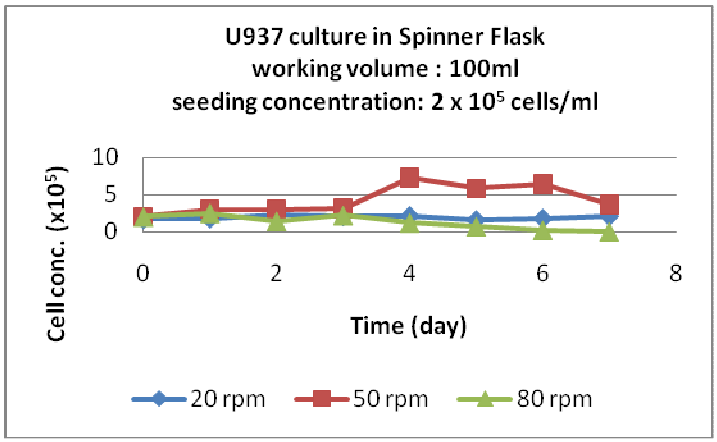

Fig 2 Comparison for U937 cells culture with different agitation speed

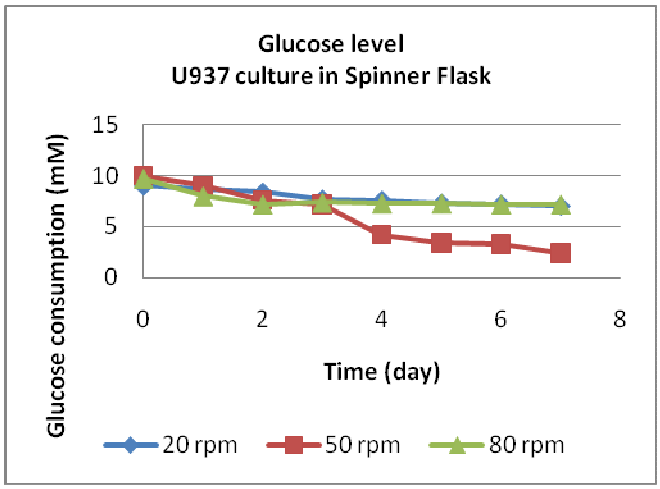

Figure 3 Glucose level analysis for U937 cells culture with different agitation speed

DISCUSSION

Experimental results show that U937 cells cannot survive in agitation culture. The death of cells in 20 rpm culture maybe from low agitation speed that may either be inadequate, leading to cell sedimentation. At 80 rpm, high speed cell shearing may be enhanced, and this will lead to cell death[1].

REFERENCES

1. Maria Irene Sanchez Cervantes, Justin Lacombe, Fernando J. Muzzio, Mario M. Alvarez. Chemical Engineering Science. *Novel bioreactor design for the culture of suspended mammalian cells. Part 1: Mixing characterization*. 2006. Volume 61. 8075-8084.

In vitro Cytotoxicity Effect of CoCrMo Alloy at Differing Carbon Compositions

M W Norsamsiah[*], H Mohamad Noor[**], A K Mohammed Rafiq[**], A M Fadzilah Adibah[*]

[*]Department of Bioprocess Engineering, Faculty of Chemical Engineering and Natural Resources, [**]Department of Materials Engineering, Faculty of Mechanical Engineering, Universiti Teknologi Malaysia, 81310 UTM Skudai, Johor, Malaysia

SUMMARY

Differing compositions of carbon in CoCrMo alloy can significantly alter the mechanical and tribological microstructure properties.[1] The carbon composition in CoCrMo alloy vary between 0.04% and 0.30%. In this study, we analysed the *in vitro* biocompability of varying carbon compositions. Since there were no signs of morphological changes, we determined the variations in cell proliferation and viability.

INTRODUCTION

Cytotoxicity is often the consequence of exposure to harmful chemicals. However, the association between the percentage of cells killed and loss of function in tissues and organs are highly variable. Cytotoxicity assays measure the loss of some cellular or intercellular structure and/or function, including cell death[1]. The toxicity effects on cell monolayers, such as cell lysis and cell morphology are usually checked after 24 and 48 hours by microscopic observation. Cell lysis can be scored by direct microscopic observation or with the use of radiolabels or trypan blue[1]. Cell growth assay is a more informative test but requires more time and skill. In this study, we compared the *in vitro* cytotoxicity effects of differing carbon contents in CoCrMo alloy.

MATERIALS AND METHODS

Medical grade CoCrMo alloys with high and low carbon compositions were cut into cylindrical bars (h=5 mm and d=5 mm).

Table 1: Materials samples composition

Element	High Carbon	Low Carbon
Carbon	0.30	0.04
Chromium	27.16	27.20
Nickel	0.16	0.18
Molybdenum	5.50	5.58
Cobalt	Bal	Bal
Ferum	0.58	0.62

U937 cells (Human Caucasian histiocytic lymphoma) (available from ECACC, catalogue number: 85011440) were cultured in RPMI 1640 supplemented with 10% fetal bovine serum (Gibco Laboratories, Grand Island, NY), 1% penicillin-streptomycin (Sigma). HC and LC CoCrMo alloys were co-cultured in suspension for 14 days until the cell viability (< 10%) at 2.5 x 10^5 cells/ml of supplemented culture media at 37ºC in a 5% humidified CO_2 incubator. The value of doubling time (t_d) was described using kinetic analysis. Statistical analyses were performed using Sigma Plot 11.0. Values were expressed as means ± SE with triplicate independent experiments.

RESULTS

From figure 1, we observed that the cell response was quite similar to that of the control cells. However, the density of cells in high carbon (HC) composition was lower than in low carbon (LC) composition. It appears that cells in general do not demonstrate obvious morphological changes between high and low carbon compositions in CoCrMo alloys.

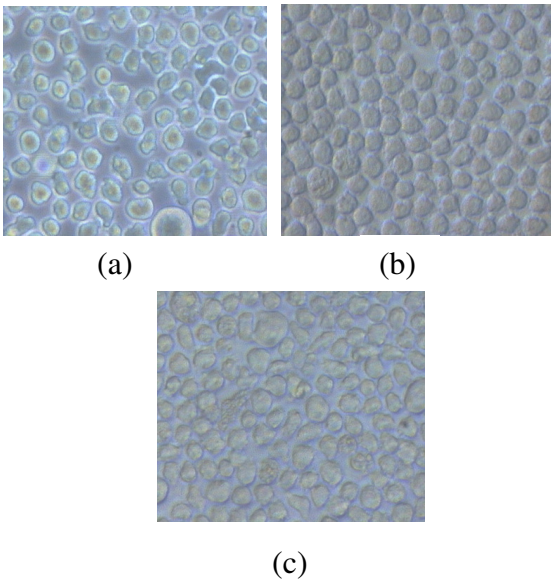

(a) (b)

(c)

Fig 1: The morphology of cells U937 (a) control sample (b) HC CoCrMo alloy and (c) LC CoCrMo alloy in cell culture medium at day 3.

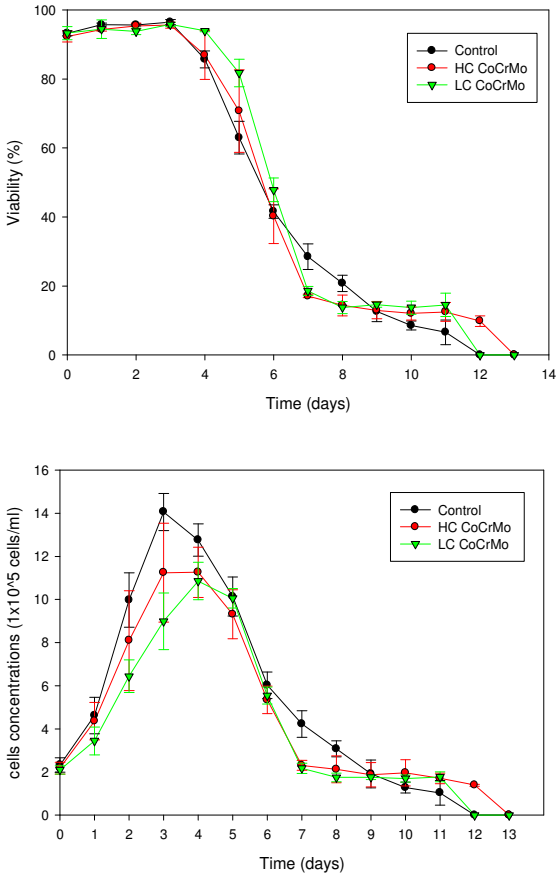

Fig 2: (a) Cell proliferation and (b) cell viability (%) of U937 cells in HC CoCrMo alloy and LC CoCrMo alloy for 14 days.

The *in vitro* evaluation of the biocompatibility of high and low carbon CoCrMo alloys were performed by cell culture and direct contact test[2]. Direct contact testing of novel biomaterials on *in vitro* cell cultures may provide an early indicator of the potential of these biomaterials. Figure 2 (a) and 2 (b) shows the result of direct contact testing of high and low carbon on U937 cell for 14 days. It is important to note, that there is no significant difference in the cytotoxicity effects of HC and LC CoCrMo alloys on U937 cells. Furthermore, there were no differences in the percentage of viable cells between both alloys. .

Table 3: The comparison of doubling time value

Variable	Doubling time
Control	2.4206
HC CoCrMo Alloy	1.92903
LC CoCrMo Alloy	1.51457

The doubling time is the period of time required for the quantity to double in size or value. We found that the doubling time of the control was highest, followed by HC CoCrMo alloy and LC CoCrMo alloy.

DISCUSSION

This study illustrates the response of cells to high and low carbon CoCrMo alloy. This preliminary cytotoxicity study shows that HC CoCrMo alloy and LC CoCrMo alloy have no significant inhibitory effects on U937 cell growth. No signs of cellular lysis were observed. The doubling time of cells show that the high carbon CoCrMo alloys is better than low carbon CoCrMo alloys. There are no morphological changes and significant cytotoxicity effects of HC and LC CoCrMo alloys to U937 cell lines based on statistical analysis. Cobalt based alloys have been widely used in orthopaedic implants because of their high hardness, exceptional corrosion resistance and wear properties[3]. This study adds to the current knowledge on the *in vitro* cytotoxicity effects of differing carbon contents in CoCrMo alloy.

REFERENCES

1. Gad SC. Safety Evaluation of Medical Devices. Marcel Dekker Inc 1997; 75 -84.
2. ASTM F 1537-07. Standard Specification for Wrought Cobalt-28Chromium-6Molybdenum Alloys for Surgical Implants. 2007; UNS R31537, UNS R31538, and UNSR31539.
3. Yan Y, Neville A, Dowson D. Biotribocorrosion – an appraisal of the time dependence of wear and corrosion interactions: I. The role of corrosion. Journal of Physics D: Applied Physics. 2007; 39, 3200-3205.

Study of Immobilized Bovine and Fish Gelatin on Carboxyl Containing Polystyrene Beads for Vero Cell Culture

Yusilawati Ahmad Nor*, Maizirwan Mel*, Hamzah Mohd Salleh*, Ng Kim Hooi, Wong C.S****

*Department of Biotechnology Engineering, Faculty of Engineering, International Islamic University Malaysia, 53100, Gombak Kuala Lumpur. **School of Arts and Science, Tunku Abdul Rahman College, 50932 Kuala Lumpur. ***Plasma Research Laboratory, Physics Department, Faculty of Science, University of Malaya, 50603 Kuala Lumpur

SUMMARY

The aim of this study is to develop a polymeric microcarrier (MC) for obtaining a higher cell density of Vero cells in spinner vessel. Different types of gelatin; bovine (BG), fish (FG), cationized bovine (CBG) and cationized fish (CFG) were covalently immobilized on carboxyl group containing polystyrene (COOH-PS). Their performance was evaluated by the cell loading test in Vero cell culture as carrier system. It was found that Vero cell has better performance on BG with highest maximum cell number at $1.45x10^5$ cell/ml with good microscopic and suspension ability; easy sampling and easy cell recovery.

INTRODUCTION

Polystyrene (PS) is widely used polymer as a core substrate for microcarriers because of its favorable properties such as low specific weight, high chemical resistance and biocompatible [1]. Gelatin has domains of arginine–glycine–aspartic acid (RGD) peptide sequences that mimic many features of the extracellular matrix (ECM) in their molecules which can be recognized as ligands that can be specifically bind with integrin on cell membranes. These properties can effectively introduce specific interaction with the cell receptor and accelerate cell attachment and spreading [2].

MATERIALS AND METHODS

Cationized gelatin was prepared by reaction of ethylenediamine and 1-ethyl-3-(3-dimethylaminopropyl) carbodiimide hydrochloride (EDC) in phosphate-buffered solution (PBS); pH adjusted to 5.0; agitated at 37^0C for 18 hr; dialyzed against double distilled water (dH_20) and freeze-dried. COOH-PS was activated by EDC (10mg/mL), and N-hydroxysuccinimide (NHS, 8mg/mL) in PBS. It was then coated with 10mg/mL gelatin solution in PBS. Three (3) g/L of COOH-PS, bovine gelatin coated PS (BGPS), cationized bovine gelatin coated PS (CBGPS), fish gelatin coated PS (FGPS) and cationized fish gelatin coated PS (CFGPS) were sterilized in PBS by autoclaving at 121°C for 15min.Vero cultures were carried out in 200mL DMEM and 10% serum in spinner vessel at 37ºC, 5% CO_2 humidified incubator. The experiments were carried for 96 hr.

RESULTS

Fig. 1 shows that the amount of amino group increased after cationization of gelatin. The amino concentration ratio of cationized gelatin to gelatin for bovine is 1.184 while the ratio of cationized gelatin to gelatin for bovine is 1.254. Results in Fig. 2 found that COOH-PS alone is suitable candidate as MC for Vero cells. However, the immobilization of gelatin (BG and FG) on the beads improved its performance in the culture by 10 fold from initial cell seeding. Fig. 2 shows that maximum cell number was obtained for BGPS with $1.45x10^5$ cell/mL followed by FGPS with $1.35x10^5$ cell/ml, CBGPS with $1.0x10^5$ cell/mL, COOH-PS with $7.5x10^4$ cell/mL and CFGPS with $2.0x10^4$ cell/mL at hour 80. Fig. 3 on the other hand shows that cell start to attach on the BGPS surface at day 1 and grown into high density on the MCs bead.

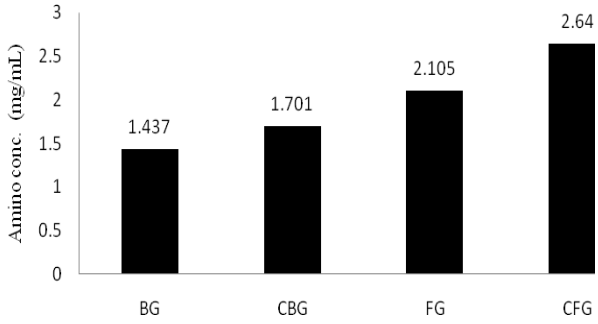

Fig. 1: Amino group content of gelatin and cationized gelatin

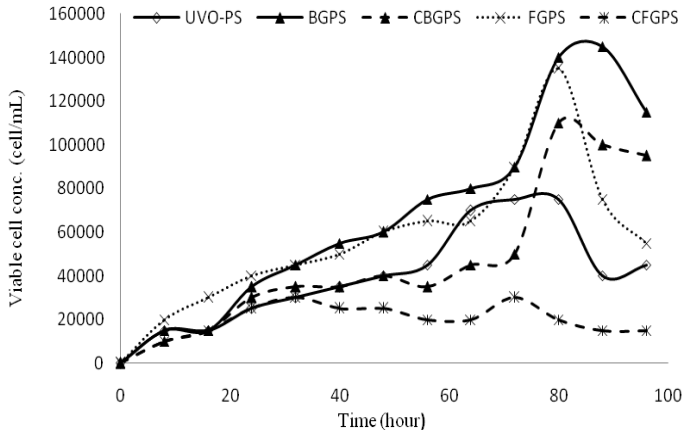

Fig. 2: Growth profile of Vero cells on different types of gelatin in spinner vessel culture

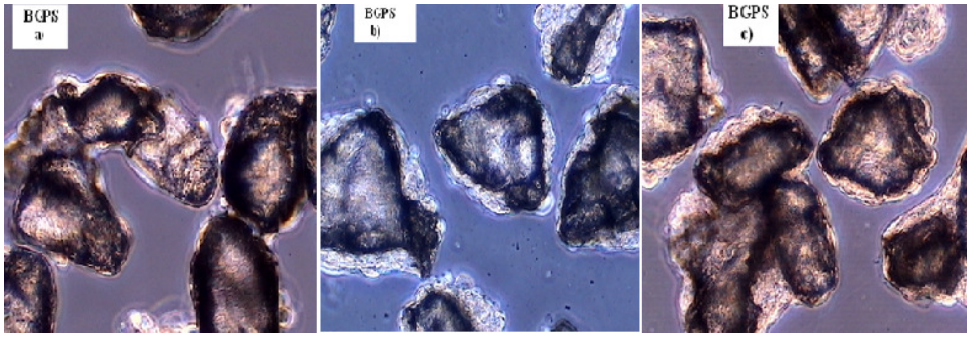

Fig. 3: Attachment of Vero cells on PS surface. Shining part represents cells, black region represent the microcarrier.

DISCUSSION

Vero cells grow much efficiently in BGPS compared to other microcarriers. This is due to the property of BG that contains integrin-binding domains which often increased the attachment of specific cells for a designed substrate in *in vitro* environment [3]. FG on the other hand is less resistance to acidic pH of the media because of low strength [4] which easily degraded the complex structure of the FG.

Reference

1. Murakami, T.N., Fukushima, Y., Hirano, Y., Tokuoka, Y., Takahashi, M. and Kawashima, N. Modification of PS films by combined treatment of ozone aeration and UV irradiation in aqueous ammonia solution for the introduction of amine and amide groups on their surface. Appl. Surf. Sci. 2005; 249: 425–432.
2. Hu, M., Kurisawa, M., Deng, R., Teo, C.M., Schumacher, A., Thong, Y.X., Wang, L., Schumacher, K.M. and Ying, J.Y. Cell immobilization in gelatin–hydroxyphenylpropionic acid hydrogel fibers. Biomaterials. 2009; 30: 3523-3531.
3. Mojovic, L. and Jovanovic, G. Biosensor forddetection of environmental and biological toxins based on fish chromatophores. Chem. Ind. 2004; 58: 99-102.
4. Haug, I.J., Draget, K.I., and Smidsrod, O. Physical and rheological properties of fish gelatin compared to mammalian gelatin. Food Hydrocolloids. 2004; 18: 203-213.

Composite of Porous Hydroxyapatite with Alumina for Bone Repair

M Rusnah, I Besar, M Reusmaazran

Materials Technology Group (MTEG), Industrial Technology Division (BTI), Malaysia Nuclear Agency, Bangi, 43000 Kajang, Selangor D.E, Malaysia

SUMMARY

Fabrication of porous HA using polyurethane form as scaffold was investigated in this study. The technique involved dipping of the foam into slurry prepared by mixing of HA+Al_2O_3 powder with PVA and Sago as the binder. Sintering was performed at 1100ºC, 1200 ºC and 1300ºC. HA powder was prepared by sol-gel precipitation method using calcium hydroxide and ortho-phosphoric acid followed by spray drying. Commercial Al_2O_3 powder was mixed with the HA powder and the binding agent comprising of sago and PVA to form the slurry. In this study, 1:1 ratio of sago:PVA was adopted successfully. The technique produced uniform pore shape. Characterization of the physical analysis, porosity, surface morphology by Scanning Electron Microscopy Analysis (SEM) and compression strength were performed. Our study revealed that porous HA+Al_2O_3 exhibited higher compression strength compared to porous HA alone and that increasing the sintering temperature increases the composite strength.

INTRODUCTION

In medical application, hydroxyapatite is commonly utilized as artificial bone, tooth roots, percutaneous devices and materials for drug delivery system [1]. Recently, the demand for synthetic bone replacement materials has increased due to a limited supply of autograft materials and the health risks associated with the use of allografts [1]. Porous hydroxyapatite has the potential to be used as synthetic bone graft material because it is bioactive and biocompatible with bone tissues [1]. For clinical success, a synthetic bone-graft material must possess an open macro-porous structure similar to that of cancellous bone, so as to promote complete penetration of bone tissues, bone marrow and blood vessels [2]. Porosity can be introduced to prevent loosening of the implant as the growth of bone into the pores provides a large interfacial area between the implant and the bone. The objective of this project is to study the use of Alumina as additives materials to strengthen porous HA.

MATERIALS AND METHODS

In this preliminary study, the commercially available Medical grad Alumina was used to mix with HA produced in our laborotary. The HA powder used in this work was synthesized by sol-gel precipitation upon mixing calcium hydroxide with orthophosphoric acid. HA powder measuring < 5µm was prepared by Spray-drying (Niro MOBILE MINOR^{TM}) then mixed with Al_2O_3 powder at 50:50 w/w plus the binder agent comprising of sago and PVA. PU sponges were used as scaffolds. Different ratio of sago:PVA was varied to determine its effect on the quality of the porous HA+Al_2O_3. PU sponges were dipped in the HA+Al_2O_3 slurries, then dried in an oven at 50 ^oC followed by organic burnout at 400^{o}C and finally, the sintered at 900^{o}C, 1000^{o}C, 1100^{o}C, 1200^{o}C and 1300^{o}C. Surface morphology was done using SEM (Leo, Oxford Instruments, 7355). The phase purity and crystallography were investigated using an XRD machine (Siemen, D5000) whereas FTIR (Perkin Elmer, Spectrum 2000) was used to detect the chemical structure. The density was calculated with the aid of a densitometer (Mirage, SD-200L).

RESULTS

Figure 2 shows that the fine particle size of Alumina is 0.43µm.

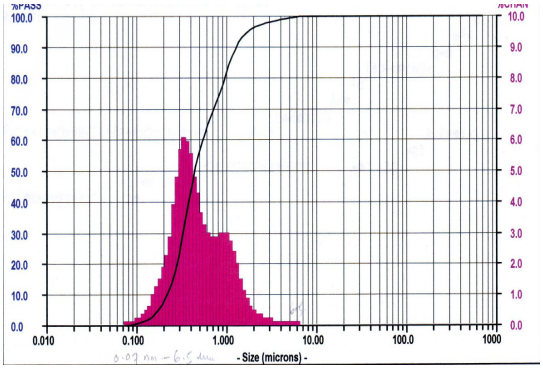

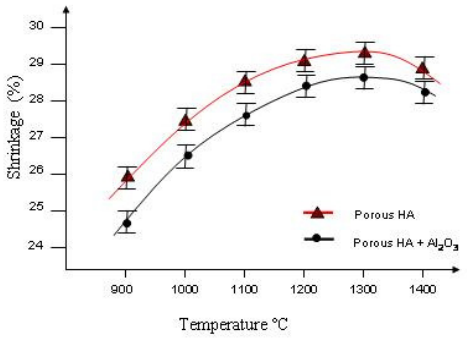

Fig 3: Shrinkage HA+Al_2O_3 with HA

Comparison of porous HA+Al_2O_3 with porous HA is shown in Figure 3. Shrinkage of porous HA (28.5%) & HA+Al_2O_3 (29.7%.) reached maximum at 1200ºC and decreased beyond 1300ºC.

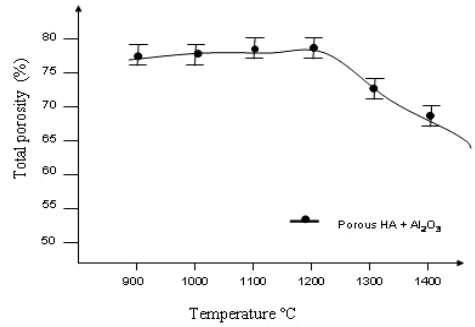

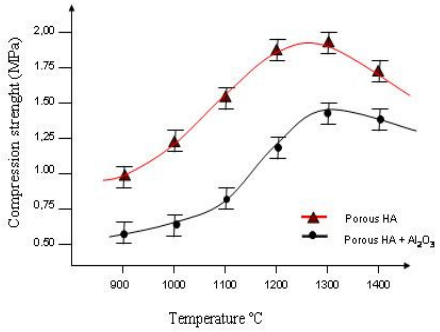

Fig 4: Total porosity vs temperature Fig 5. Compression strength vs temperature

Compressive strength, porosity and apparent density are interrelated. At lower temperature i.e. between 900 to 1200°C, the presence of micro porosities (Figure 4) in porous HA+AL_2O_3 samples contributed to higher total porosity. Higher temperature (1300 to 1400°C) resulted in HA+Al_2O_3 struts that was covered with micro pores. The apparent density and compressive strength of porous HA was also decreased (Figure 5).

DISCUSSION AND CONCLUSION

After sintering the porous HA+AL_2O_3 sample at 900°C, the strength obtained is around 0.53 MPa, increased to 1.45 MPa at 1300°C and decreased to 1.3Mpa at 1400ºC. The compressive strength increased with the sintering temperature which corresponded with the increasing samples density and decreasing porosity. The obvious increase in compressive strength is due to the great reduction of porosity at this range of sintering temperatures. At higher sintering temperatures, porosity was constant and compressive strength was not greatly affected. In all cases, porosity was found to decrease with increasing of sintering temperature. No change in shrinkages occurred and complete grain growth at 1300°C led to constant porosity beyond this sintering temperature. The shrinkages of porous HA samples were greatly related to the porosity obtained. Constant shrinkages was also observed after the temperature of 1300°C, indicating a strong relationship between porosity and shrinkage. Shrinkage that occurred at lower sintering temperatures dramatically reduced the porosity but porosity remained constant at higher temperature. This phenomenon leads to the variation in compressive strength of porous HA. XRD patterns of porous HA sintered at different temperature are shown in Figure 3. The XRD patterns at low sintering temperatures (1000 to 1200°C), indicated the presence of only pure phase HA and a small percentage of CaO which was considered normal in producing HA. Other phase such as tri-calcium phosphate was detected at 1300°C and tetra-calcium phosphate and calcium pyrophosphate phases were present at higher sintering temperature. At the room temperature, HA is in an amorphous calcium phosphate (ACP) phase and converts to calcium deficient hydroxyapatite (CDHA) when the sintering temperature reaches 700°C [3]. At this temperature, HA begin to gain its stoichiometry.Porosity and compressive strength of porous HA are very much affected by the sintering temperature. Higher sintering temperature produced higher compressive strength in porous HA that is associated with decreasing porosity and also grain growth of porous HA struts. Addition of Al_2O_3 as composite to porous Ha did not increase compressive strength compared to porous Ha.

REFERENCES

1. Ryu, H. S., Kim, S. J., Kim, J. H., Kim H. and Hong K. S., 2004. Fabrication of 1-dimensional porous hydroxyapatite and evaluation of its osteoconductivity. J. Materials Science: Material in Medicine 15 : 276-273.
2. Tampieri, A., Celotti, G., Szontagh, F. & Landi E. 1997. Sintering and characterization of HA and TCP bioceramics with control of their strength and phase purity. J. Materials Science: Material in Medicine 8: 29-37.
3. Jiming Z., Xingdong, Z. & Jiyong, C. 1993. High temperature characteristic of synthetic hydroxyapatite. J. Materials Science: Material in Medicine 4: 83-85.

Nanotechnology and Biomimetics in Tissue Engineering and Regenerative Medicine

I C Gebeshuber [*,,***], M O Macqueen[****], B Y Majlis[*]**

[*]Universiti Kebangsaan Malaysia, Institute of Microengineering and Nanoelectronics, 43600 UKM Bangi, Malaysia. [**]Institute of Applied Physics, Vienna University of Technology, Wiedner Hauptstrasse 8-10/134, 1040 Wien, Austria. [***]TU BIONIK Center of Excellence, Getreidemarkt 9/166, 1060 Wien, Austria. [****]Aramis Technologies, 57000 Kuala Lumpur, Malaysia

SUMMARY

Two prominent research areas at the meeting place of life sciences with engineering and physics are nanotechnology and biomimetics. Nanotechnology is the science and technology of designing, producing, and using structures and devices having functional units at length scales of about 100 millionth of a millimetre (100 nanometres) or less. One of the fascinating aspects of nanotechnology is that on the nanometer scale all natural sciences meet and intertwine. The life science meet physics as well as engineering, chemistry, materials science and computational approaches, which altogether communicate and are closely linked. This inherent interdisciplinarity of nanotechnology offers enormous potential for fruitful cross-fertilisation in specialist areas.

Biomimetics deals with knowledge transfer of deep principles from animated nature to medicine and technology. Nature excels at combining materials, structures and processes. Planarian worms for example can re-grow body parts - including a whole head and brain. Investigations of animated nature on the nanoscale have wide-ranging implications for the understanding of processes in healthy and health impaired living beings and yield novel approaches in engineering and medicine. The foundations of both areas are presented and current research methodologies and results relevant to tissue engineering and regenerative medicine are introduced. Examples illustrating these points include biomimetic biocompatible scaffolds for tissue engineering, biomimetic nanocoated surfaces that promote osteoblast cell adhesion and a biomimetic root canal that stimulates dentin formation.

Magnetic Nanoparticle-based Tagging of Mechanosensors for Bone Tissue Engineering

A J El Haj

Institute of Science and Technology in Medicine, Keele University Medical School, UK

SUMMARY

A major component of constructing connective tissues for regeneration and repair is the control of cell proliferation and activity. Mechanosensors in membranes are key regulators in the differentiation, proliferation and activity of bone cells. Activation and regulation of these mechanosensors has been proposed as a means by which engineering of tissues may be enhanced. Generating functional bone and connective tissue in vitro relies on culture environments which condition the tissue prior to implantation. Multiple protocols for the use of bioreactors which exert forces such as fluid flow and compression have been proposed. In this presentation, we describe a different approach where we target specific mechanosensors directly on human bone cell membranes within 3D constructs. By controlling the mechanical environment of the cells within the construct, we are no longer reliant on using strong materials which are capable of withstanding significant loading for bone tissue engineering. Hence, we aim to increase the turnover relationship between matrix and more rapidly degrading scaffolds in response to mechanical stimulation. Using a magnetic force bioreactor developed in our lab, we describe our investigations into the binding of magnetic nanoparticles to receptor sites on the membrane of cells. By applying time-varying magnetic fields, we can generate forces on these receptors which result in downstream changes in gene expression and enhanced matrix production. A comparison of data generated from the type of receptor tagged such as integrins, ion channels and growth factor receptor sites will be described. Control of stem cell differentiation is crucial to development of stem cell therapy strategies. The magnetic particle tagging technique has been applied to human mesenchymal stem cells in monolayer culture, 3D configurations in vitro and implanted in animals *in vivo*. We have demonstrated an upregulation of differentiation markers such as osterix, cbfa1 and up regulation of extracellular matrix in response to remote magnetic tagging of receptors. The magnetic nanoparticle technology can also be applied directly *in vivo* in animal models and ultimately in clinical treatments. We describe recent investigations into localisation of stem cells *in vivo* using magnetic tagging and tagging of key receptors for manipulation *in vitro* and *in vivo* for use in regenerative medicine therapies.

Rapid Prototyping Technique – Today's and Tomorrow's Technology to Develop 3D Tissue Engineering Scaffold

M E Hoque

Department of Mechanical, Materials & Manufacturing Engineering, University of Nottingham Malaysia Campus

SUMMARY

Besides biocompatibility and bioresorbability, architectural controllability and reproducibility of 3D tissue engineering (TE) scaffolds have increasingly been of high importance. To date, a wide range of conventional techniques have been extensively used to develop scaffolds using numerous materials. In spite of providing the scaffolds with various characteristics, these techniques inherit some fundamental limitations such as lack of full control over the pore morphology, connectivity, reproducibility and consequently, biomechanical properties. Rapid Prototyping (RP) technique, a layer-by-layer additive approach, offers a unique opportunity to develop scaffold with customized biomechanical properties (in terms of structural integrity, strength and micro-environment) similar to the organ or tissue to be repaired/replaced as close as possible. This paper provides a brief overview of various scaffold fabrication RP technique, and elaborates on an in-house built desktop robot based rapid prototyping (DRBRP) technique. The DRBRP technique enables developing scaffolds with various biopolymers and micro-architectures producing range of biomechanical properties aiming to cater for wider tissue engineering applications.

Different Assessment Modalities (Radiography, Urodynamic, Ultrasonography) for the Evaluation of Urinary Bladder Reconstrustruction

A S Salah*, M H Ng **, M Z Zulkifili*, C C K Ho*, S Ismail*, B H I Ruszymah**

*Department of Surgery, UKM Medical Centre, **Tissue Engineering Centre, UKM Medical Centre

SUMMARY

Patients with urinary bladder diseases, either congenital or acquired (eg. trauma or carcinoma) require partial or subtotal urinary reconstruction. A successful reconstruction should be confirmed by the measurement and evaluations of returned bladder structure and functions to normal values. In this study,different assessment modalities, specifically, radiography(CT scan), ultrasound, and urodynamic were used on Sprague Dawley rats with normal urinary bladder. Radiolography(CT scan) and ultrasonography provided structural information that was correlated with functional parameters provided byurodynamic studies.This study demonstrated that the different assessment modalities complimented each other and the findings correlated well. In combination, they provided a total assessment of urinary structure and functions i.e. normal urinary bladder volume, bladder filling pressure, voiding pressure, bladder shape, outline border, configuration, location and dimension.

MATERIAL AND METHODS

Female Sprague Dawely rats weighing 250-280g were used for urinary bladder structure and functions assessment by radiography, ultrasonography, and urodynamic studies. Animals wereanesthetizedusing 0.1ml KTX mixture (Ketamine, Zoletil, Xylazine) via IV injections prior to the assessments. X-ray and subsequent 3D scanning was performed using Skyscan 1076 high resolution *in vivo* scanner, (Belgium). Plain x-ray(without contrast agent) was initially taken for detection of any pathological calcification followed by cystography, the introduction of contrast agent, Omnipaque (350µg/ml, Ireland)(50:50 contrast: normal saline; using 3Fr urethral catheters). 3D scanning was performed at a resolution of 9µm per section. Prior to the ultrasound examination, animal was clean shaved at the abdominal area and the area layered with a generous amount of conductive gel. The bladder was filled with normal saline using 3F urethral catheters. Ultrasound images were taken using SonoSite (Bothell, USA). Probe used is a linear multifrequency probe at 10Mhz. In urodynamic study, 6Frtwin lumen urodynamic catheter was used for directintravesical measurement by insertion of the catheter throughsuprapubic incision. The pressure probe was inserted into the**TRITON™ Wireless Urodynamics Systems** (Laborie Medical Technologies Corp, Canada)

RESULTS

Initial X-ray before contrast introduction showed no bony abnormalities or pathological calcifications. Cystography revealed a rat urinary bladder that was oval and fusiform in shape with a regular smooth outline, was located centrally at lower abdominal segment with bladder neck and urethra caudally located (Figure 1a). 3D reconstruction of the bladder revealed a regular bladder configuration (Figure 1b) and allows accurate calculation of bladder volume (1.5ml) using preinstalled software.

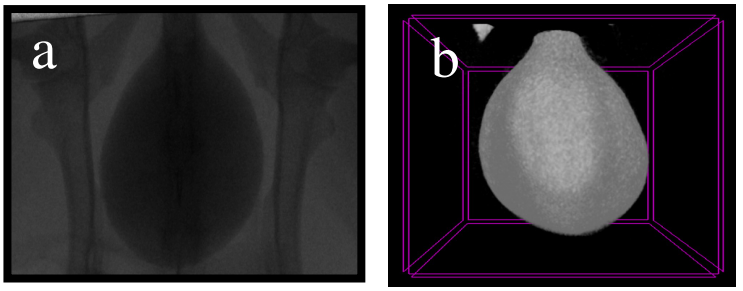

Fig 1 a)Urinary bladder x-ray, contrast,(A-P) view ;

b) Urinary bladder 3D scan

Ultrasonography provided real time image of urinary bladder and additional parameters compared to x-ray such as wall thickness. It revealed a bladder that was round (cross section) and fusiform (longitudinal section), with a hypoechoic lumen bladder volume measured approximately 1.3ml using the prolate ellipsoid method based on the formula: volume = length x width x heigth x 0.52 on two dimension[1]. Post-voiding residual urine was 0.88ml. Wall

thickness was 1mm at anterior aspect and 2mm at posterior aspect and near bladder neck.

(a)

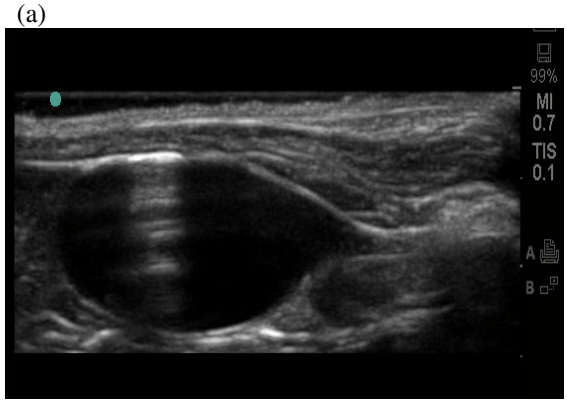

(b)

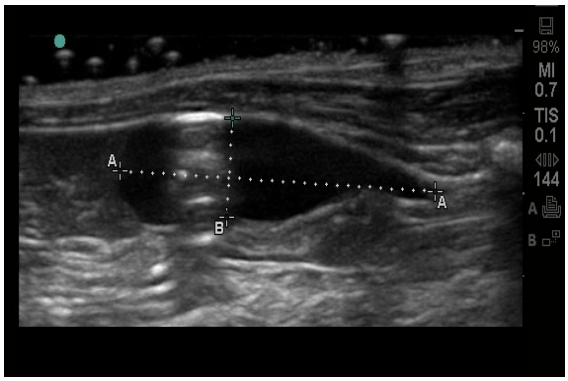

Figure 2 Ultrasonography of
a) full baldder longitudinal section;
b) post- voiding bladder with residual urine

In urodynamic study, the infusion rate under gravitational force was 0.05ml/sec and the maximum saline filled before involuntary voiding took place (bladder volume) measured manually was 1.42ml. The urodynamic machine measured an intravesical filling pressure that was low (5-6cmH2O) and not rising during bladder filling allowing it to accommodate urine to full capacity and reflecting proper bladder compliance followed by a sudden rise in pressure i.e. voiding pressure(18-19 cmH2O) during bladder contraction and urine voiding (Figure 3).

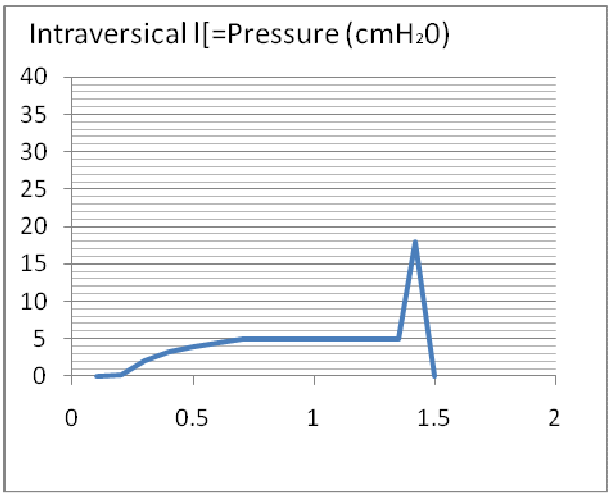

Figure 3.Urodynamic Study Diagram

DISCUSSION AND CONCLUSION

The three assessment modalities complemented each other to provide an overall and complete assessment of the urinary bladder structure and functions of a normal rat.Bladder volume of normal rat measured using the three methods ranged between 1.3-1.5ml. These baseline data will be used as a reference to evaluate the success of urinary bladder reconstruction in our further studies.

REFERENCES

1. Dicuio M, Pomara G, MenchiniFabris F, Ales V, Dahlstrand C, Morelli G. Measurements of urinary bladder volume: comparison of five ultrasound calculation methods in volunteers.Arch ItalUrolAndrol. 2005 Mar;77(1):60-2.

In Vitro Evaluation of Dye Retention and Viability Using PKH26 in Bone Marrow and Adipose Stem Cell for Cell Tracking

C Ude Chinedu, **B S Shamsul, *Ng Min Hwei[1], ***H C Chen, **Y Nur Hamdan, *,*B H I Ruszymah**

[*]Tissue Engineering Centre, University Kebangsaan Malaysia Medical Centre. **Department of Orthopedic and Traumatology, UKMMC Malaysia. ***Faculty of Veterinary Medicine, University Putra Malaysia. ****[4]Department of Physiology, Medical Faculty University Kebangsaan Malaysia

SUMMARY

Stem cells from sheep bone marrow and adipose tissue were labeled with different concentrations of PKH26 dye and cultured in FD + 10% FBS medium in order to evaluate their dye retention capacity with passaging and also their viability after the staining. Stem cells were derived from two bone marrow (BMSC) and five adipose tissues (ADSC) samples. Cells of passage 2-5 were labeled with three different concentrations of PKH26. i) $8x10^{-6}$ M; ii) $4X10^{-6}$ M and iii) $2X10^{-6}$ M. All samples were retained PKH26 dye for the subsequent six passages which spanned between 44-53 days and acquired a mean cumulative population doubling of 12–15. Compared to BMSCs, ADSCs have greater ability to pick up the stain and retain it as compared to BMSCs. However, ADSCs demonstrate more cytotoxic effect of the dye at higher concentration. Both BMSCs and ADSCs had more than 90% positivity and a cell viability of more than 80% immediately after staining with PKH26 at $8x10^{-6}$M and $2x10^{-3}$M respectively. Twenty four hours later, viability of ADSCs reduced to 50-60% while the BMSC maintained the viability of 90%.

INTRODUCTION

Stem cell therapy promises a therapeutic option for many diseases. As the field of cellular transplantation matures, there is the need to longitudinally track and evaluate the functional effects of transplanted cells. Although many human studies have been initiated in recent years however the rapid translation into clinical medicine has left many questions unresolved, which underscores the importance of using molecular based imaging modalities to monitor stem cell survival and behavior *in vivo* [1]. PKH26 is a lipophilic dye and it has been used for multiple purposes in in-vitro tracking of various kinds of cells. This dye has a half-life of elution from rabbit red blood cells of greater than 100 days in vivo [2]. Furthermore, PKH26 is easily detected by conventional fluorescent microscopy and stably incorporated into the cell membrane; allowing for the proliferation assessment. Similar to other cell tracking dyes, PKH26 has cytotoxic effect on cell which depends on the type of cell stained; the concentration of dye used and the population of cell stained [3].

MATERIALS AND METHODS

Bone Marrow samples were harvested from the iliac crest of the sheep by the aid of heparinised 50ml syringe and a bone marrow trocar [4]. Adipose tissues were harvested from the right periscapular area of sheep. The cells were labeled with the PKH26 dye according to the manufacturer's protocols. Cell counts were done via hemocytometer and viability by trypan blue exclusion prior and after the staining. The mean florescence retention was determined with the florescence microscope [5]. The cells were cultured in FD + 10% FBS medium upon staining, seeded with different densities; trypsinized and passaged when they averaged 90% confluence. The expansion and culture of the cells were terminated when they had lost all the florescence.

RESULTS

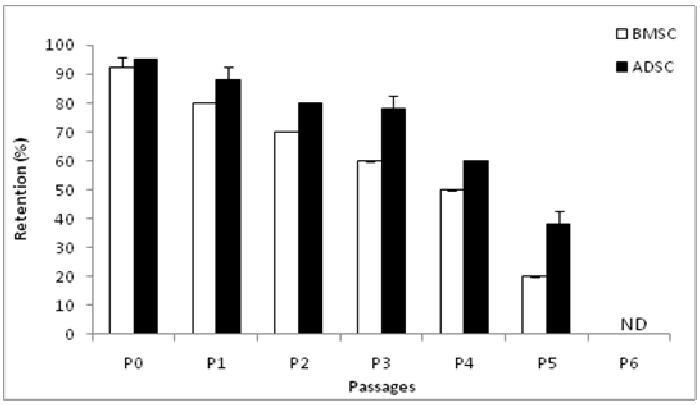

Fig.1. PKH26 florescence retention of BMSCs and ADSCs in subsequent passages for an average period of 49 days. (p= passages; ND= no detection)

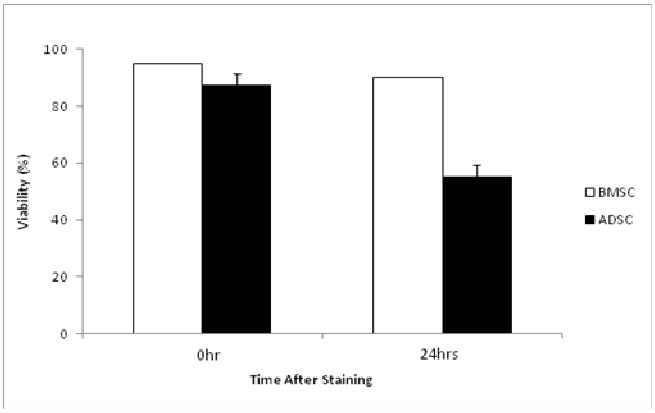

Fig.2. Viability of BMSCs and ADSCs upon staining and after 24hrs..

DISCUSSION

This work reflects an effort to longitudinally track and evaluate the functional effects of transplanted cells *in vitro*. Both BMSCs and ADSCs were able to retain their florescence for an average period of 49 days, having a mean cumulative population doubling of 14.4. The two cell type displayed differential ability to pick up staining and susceptibility to cytotoxic effect of the dye. The results implied that BMSCs are less ready to pick up PKH26 dye; has higher resistance to the cytotoxicity effect of the dye and has less ability to retain the dye. The ADSC on the other hand were more readily to pick up the dye even at very low concentration; with higher susceptibility to the cytotoxicity effect of the dye and has greater ability to retain the dye. Further investigation and clarification on this work could be done with the aid of live imaging experiments.

REFERENCES

1. Jeremy Pearl BS and Joseph C. Wu. Seeing is Believing: Tracking Cells to Determine the Effect of Transplantation .Seminar in Thoracic and Cardiovascular Surgery Vol.20, Issue 2, Summer 2008, pp 102-9
2. Sigma et al. Staining optimization for PKH Dyes. Research, 53, 2360 (1993)
3. Poon, R.Y et al. In: Living colour; Flow Cytometry and Cell Sorting Protocols. (Diamond, R.A Demaggio, S.eds) New York: Springer Verlag, P. 302-352(2000.)
4. Darko Bosnakveski, Morimichi Mezuno, Gonhyung Kin, Taketo Ishiguro Asakiro Okumura, Toshihiko Iwanaga, Tsuyoshikadosawa, and Toru Ujinaga; Chondrocyte Differentiation of Bovine Bone Marrow Mesenchymal Stem Cell in Pellet Culture System. Journal of Experimental Haematology. 2004; volume 32 pp 502-509.
5 Qiang Yang, Jiang Peng, Quanyi Guo, Jingxiang Huang, Li Zhang, Juo Yao, Fei Yang, Shenguo Wang, Wenjing Xu, Aiyuan Wang, Shibi Lu. A Cartilage ECM-Derived 3-D Porous Acellular Matrix Scaffold for In vitro Cartilage Tissue Engineering with PKH 26-Labeled Chondrogenic Bone Marrow-Derived Mesenchymal Stem Cells. Biomaterials 29(2008) 2378-2387.

Designing New Strategies for Delivering Cell Therapies into the Clinic

A J El Haj

Institute of Science and Technology in Medicine, Keele University Medical School, United Kingdom

SUMMARY

The use of stem cells as a therapeutic tool provides great promise to many clinical conditions. The challenges lie in designing a suitable strategy for treatment and defining methods for control of cells once delivered into the patient. Therapies can include delivery of nascent engineered 'tissues' into the body after culture *in vitro* or delivery of cells into appropriate conditions in the patient which enables new tissue growth. In both cases, the treatment requires an understanding of the tissue behaviour, function and architecture to allow for good clinical outcomes. In this presentation, the challenges of cell therapies are introduced and the novel solutions for controlling cells *in vitro* and *in vivo* from our laboratory are described. An important aspect of the development of new treatments is the ability to define the outcome more closely with cellular resolution. New imaging modalities are allowing us to non-invasively characterise the success of our implants and our developments in this area will be outlined. This is essential for regulatory bodies in accepting new treatments and industrial commercialisation. Finally, preliminary cell therapies have begun to be utilised in the clinic in orthopaedics and the latest clinical treatments within our hospital will be described.

Mesenchymal Stem Cell Scale-Up for Cartilage Engineering

Tunku Kamarul Zaman

Tissue Engineering Group (TEG), National Orthopaedic Centre of Excellence for Research and Learning (NOCERAL), University of Malaya, Lembah Pantai 50603 Kuala Lumpur

SUMMARY

The use of tissue engineering techniques to repair damaged cartilage has received tremendous attention globally owing to its promising results in a number of established clinical trials. The advances in the scaffold designs, biochemical promoters and other laboratory techniques have enabled better methods for cartilage to be engineered in both *in vitro* and *in vivo* environments. Among the various components important for cartilage engineering, the cells used in these engineered constructs remains the key factor to a successful cartilage design. Although the use of autologous chondrocytes in cartilage engineering has been well established since the mid 1980s, the major problem of relatively poor proliferation capacity and limited life span of these cells remains an unresolved issue. Mesenchymal stem cells (MSCs) have been recognised as an attractive alternative candidate for use in biological cell-based therapies, especially in cartilage engineering. These cells appear to be easily harvested and have superior proliferation rates while maintaining the ability to retain their mesenchymal multilineage differentiation potential. These are desirable qualities which have resulted in MSCs being a focus of research interest among many tissue engineers who are in the quest to produce better tissue design. However, the question remains: is the performance of MSCs compatible with the expectations of many in the field of tissue engineering, or, is the MSCs' role in this domain just another fad that will wither with time? While there have been many basic science research studies reporting good results related to the use of MSCs in cartilage repair, there was only one true clinical trial comparing autologous chondrocytes to MSCs. This study demonstrated that the use of MSCs did not provide the expected improvement in various clinical outcomes, as compared to the autologous chondrocyte treatment. This has led to the perception that, perhaps, the true benefits of MSCs may have been overstated, generating a false impression of its true value in cartilage construct designs. In this presentation, a detailed analysis of current research related to cartilage engineering will be discussed, emphasizing on major research findings related to this area, with the aim to provide a clearer picture regarding the role of MSCs in cartilage engineering.

Tissue Engineering of the Cornea in Rabbit Model

A G Norzana[*], C H Jemaima[**], K H Chua[***], A R Ropilah[**], O Fauziah[*******], W N Wan Zurinah[****], A A Raymond[*****], B H I Ruszymah[*,******]**

[*]Department of Anatomy, [**]Department of Ophthalmology, [***]Department of Physiology, [****]Department of Biochemistry, [*****]Department of Medicine, [******]Tissue Engineering Centre, Faculty of Medicine, Universiti Kebangsaan Malaysia, [*******]Department of Anatomy, Faculty of Medicine, Universiti Putra Malaysia

SUMMARY

Expansion of corneal cells while maintaining their phenotypes is vital prior to corneal construct formation and transplantation. It is essential to have tissue engineered corneal construct with cells that possess a long term regenerative capacity for cellular renewal and replacement of the tissue. Limbus, has long been identified as the stem cell pool for corneal epithelial cells and expansion of these cells using 3T3-feeder layer has been ubiquitously employed by most researchers. Xenogeneic microchimerism, xenozoonosis and tumorigenesis remain theoretical possibilities in light of potential mutagenic effects of gamma irradiation and mitomycin C-treated feeder layer, which both affect the cellular DNA. Hence, the exclusion of xenogeneic feeder layer during cultivation of corneal cells whilst maintaining its progenitor characteristics is of paramount importance in corneal tissue engineering. Here, we have demonstrated corneal epithelial and keratocytes could be culture expanded from small limbal biopsy without feeder layer by employing co-culture and differential trypsinization methods. Purity of each corneal cell culture after separation was established via gene expression analysis and contra-medium cultivation analysis. Sufficient corneal cells were then homogenously incorporated into autologous fibrin to form tissue engineered corneal substitute. Autologous transplantation of tissue engineered corneal substitute revealed regeneration and restoration of corneal surface with ocular transparency achieved at 3 months post-transplantation in lamellar keratectomy rabbit model. Corneas in lamellar keratectomized rabbits with no transplantation showed significant thinning whereas corneas in rabbits with transplanted fibrin construct devoid of cells showed significant thickening and scarring. This novel tissue engineered corneal substitute utilizing fibrin has enormous clinical potential as it is not only biocompatible and biodegradable but also possess immunological integrity as all the cells and biomaterial are autologously derived from the subject. The details of the process, *in vitro* and *in vivo* studies will be presented.